

MICROCOPY RESOLUTION TEST CHART
NATIONAL BUREAU OF STANDARDS 1963-A

UNCLASSIFIED

SECURITY CLASSIFICATION

AD-A185 387

DTIC FILE COPY

REPORT PAGE

2

1a. REPORT SECURITY CLASSIFICATION UNCLASSIFIED

2a. SECURITY CLASSIFICATION AUTHORITY SELECTED

2b. DECLASSIFICATION/DOWNGRADING SCHEDULE OCT 01 1987

4. PERFORMING ORGANIZATION REPORT NUMBER(S) CD 5. MONITORING ORGANIZATION REPORT NUMBER(S) AFOSR-TR-87-1006

6a. NAME OF PERFORMING ORGANIZATION WEA

6b. OFFICE SYMBOL (If applicable)

7a. NAME OF MONITORING ORGANIZATION AFOSR/NA

6c. ADDRESS (City, State and ZIP Code) P.O. Box 260, MIT Branch Cambridge, MA 02139

7b. ADDRESS (City, State and ZIP Code) Bldg 410 Bolling AFB DC 20332-6448

8a. NAME OF FUNDING/SPONSORING ORGANIZATION AIR FORCE OFFICE OF SCIENTIFIC RESEARCH

8b. OFFICE SYMBOL (If applicable) AFOSR/NA

9. PROCUREMENT INSTRUMENT IDENTIFICATION NUMBER F49620-85-0148

8c. ADDRESS (City, State and ZIP Code) Bldg 410 BOLLING AFB, DC 20332-6448

10. SOURCE OF FUNDING NOS

11. TITLE (Include Security Classification) COMPUTATION OF NATURAL FREQUENCIES OF PLANAR LATTICE STRUCTURE-UNCLASSIFIED

12. PERSONAL AUTHOR(S) James H. Williams, Jr. and Raymond J. Nagem

13a. TYPE OF REPORT TECHNICAL

13b. TIME COVERED FROM 1 Sept 85 to 1 Mar 87

14. DATE OF REPORT (Yr., Mo., Day) 1987, March, 1

15. PAGE COUNT 65

16. SUPPLEMENTARY NOTATION

COSATI CODES		
FIELD	GROUP	SUB GR

18. SUBJECT TERMS (Continue on reverse if necessary and identify by block number) LARGE SPACE STRUCTURES TRANSFER MATRICES NATURAL FREQUENCIES

19. ABSTRACT (Continue on reverse if necessary and identify by block number) Transfer matrices and joint coupling matrices are used to compute natural frequencies of vibration of a five-bay planar lattice structure. The method of analysis may be applied to general two and three-dimensional lattices. The necessary numerical computations may be performed easily with a personal computer. Numerical results for the first twenty-five nonzero natural frequencies of the five-bay planar lattice structure are given for the case when the members of the lattice are modeled as Bernoulli-Euler beams, and for the case when the members of the lattice are modeled as Timoshenko beams. The maximum difference in the computed natural frequencies of the two models occurs in the twenty-fifth mode and is less than one-half of one percent. The natural frequencies obtained here agree within six percent with the natural frequencies obtained in a previous analysis using a finite element method and an experimental modal analysis.

20. DISTRIBUTION/AVAILABILITY OF ABSTRACT UNCLASSIFIED/UNLIMITED [X] SAME AS RPT [] DTIC USERS []

21. ABSTRACT SECURITY CLASSIFICATION UNCLASSIFIED

22a. NAME OF RESPONSIBLE INDIVIDUAL ANTHONY K. AMOS

22b. TELEPHONE NUMBER (Include Area Code) 202/767-4937

22c. OFFICE SYMBOL AFOSR/NA

AFOSR-TR. S7-1006

ACKNOWLEDGMENTS

The Air Force Office of Scientific Research (Project Monitor, Dr. Anthony K. Amos) is gratefully acknowledged for its support of this research.

NOTICE

This document was prepared under the sponsorship of the Air Force. Neither the US Government nor any person acting on behalf of the US Government assumes any liability resulting from the use of the information contained in this document. This notice is intended to cover WEA as well.

INTRODUCTION

In a previous series of papers [1-5], matrix methods for linear dynamic analyses of lattice structures are developed. A lattice structure, in this context, is defined to be an idealized network of one-dimensional members which are connected by joints. In this paper, transfer matrices and joint coupling matrices are used to compute the natural frequencies of vibration of a five-bay planar lattice structure. The method of analysis is applicable to general two and three-dimensional lattices. The necessary numerical computations may be performed easily using a personal computer. Numerical results for the first twenty-five nonzero natural frequencies of the five-bay lattice structure are given for the case when the members of the lattice are modeled as Bernoulli-Euler beams, and for the case when the lattice members are modeled as Timoshenko beams. The results obtained here are compared with the results of a previous analysis [6] using a finite element method and an experimental modal analysis. A short discussion of the results and of some potential applications of the type of analysis presented here is given.



Accession For	
NHS CRA&I	<input checked="" type="checkbox"/>
DRG IER	<input type="checkbox"/>
...	<input type="checkbox"/>
By	
A-1	

ANALYSIS

Lattice Structure and Model

The lattice structure considered here is shown in Fig. 1. The lattice is machined from a single piece of aluminum, and contains no welds or fasteners.

The model used here to analyze the lattice structure of Fig. 1 is shown in Fig. 2. The structure is modeled as an idealized lattice of one-dimensional members which are connected by joints. It is assumed that the members and joints can move only in the plane of the structure, and that all motions are small.

The joints of the lattice model are labeled 1 through 12 as shown in Fig. 2. It is assumed that each joint is rigid, and that each connection between a joint and a beam is rigid. It is also assumed that each joint is massless and has no spatial extent. The assumptions that the joints are massless and have no spatial extent are made only for convenience; some comments about the analysis of joints with mass and/or spatial extent are given below.

It is assumed that all members of the lattice model of Fig. 2 are identical, and that each member can extend (and contract) axially and bend flexurally. It is also assumed that the axial and flexural motions are uncoupled. Two different member models are used. In the first model, hereafter called the Bernoulli-Euler beam model, the lattice members are modeled as classical longitudinal rods for axial motions and as Bernoulli-Euler beams for flexural motions. In the second model, hereafter called the Timoshenko beam model, the lattice members are modeled as classical longitudinal rods for axial motions and as Timoshenko beams for flexural

motions. In both models, the state vector at any point x of a lattice member is of the form

$$\underline{z}(x,t) = \begin{Bmatrix} u(x,t) \\ v(x,t) \\ \psi(x,t) \\ M(x,t) \\ V(x,t) \\ F(x,t) \end{Bmatrix} \quad (1)$$

where $u(x,t)$ is the longitudinal displacement of the member, $v(x,t)$ is the transverse displacement of the member, $\psi(x,t)$ is the rotation of the member, $M(x,t)$ is the bending moment in the member, $V(x,t)$ is the shear force in the member, $F(x,t)$ is the axial force in the member, x is a spatial coordinate which extends along the length of the member and t is time. The components of the state vector and the sign convention adopted here for the components of the state vector are shown in Fig. 3. Local coordinate directions x_i ($i = 1, 2, \dots, 16$) are assigned to the lattice members as shown in Fig. 2.

Joint Coupling Matrix Relationships

The Fourier transforms \bar{z}_1 and \bar{z}_2 of the state vectors z_1 and z_2 shown in Fig. 2 are related by an equation of the form [3]

$$\underline{B}_1(\omega) \begin{Bmatrix} \bar{z}_1 \\ \bar{z}_2 \end{Bmatrix} = \underline{0} \quad (2)$$

where $\underline{B}_1(\omega)$ is the joint coupling matrix of joint 1. Eqn. (2) is the joint coupling matrix relationship for joint 1. Joint coupling matrix relationships for joints 2 through 12 can be written in a similar manner as

$$\underline{B}_2(\omega) \begin{Bmatrix} \underline{z}_3 \\ \underline{z}_4 \end{Bmatrix} = \underline{0} \quad (3)$$

$$\underline{B}_3(\omega) \begin{Bmatrix} \underline{z}_5 \\ \underline{z}_6 \\ \underline{z}_7 \end{Bmatrix} = \underline{0} \quad (4)$$

$$\underline{B}_4(\omega) \begin{Bmatrix} \underline{z}_8 \\ \underline{z}_9 \\ \underline{z}_{10} \end{Bmatrix} = \underline{0} \quad (5)$$

$$\underline{B}_5(\omega) \begin{Bmatrix} \underline{z}_{11} \\ \underline{z}_{12} \\ \underline{z}_{13} \end{Bmatrix} = \underline{0} \quad (6)$$

$$\underline{B}_6(\omega) \begin{Bmatrix} \underline{z}_{14} \\ \underline{z}_{15} \\ \underline{z}_{16} \end{Bmatrix} = \underline{0} \quad (7)$$

$$\underline{B}_7(\omega) \begin{Bmatrix} \bar{z}_{17} \\ \bar{z}_{18} \\ \bar{z}_{19} \end{Bmatrix} = \underline{0} \quad (8)$$

$$\underline{B}_8(\omega) \begin{Bmatrix} \bar{z}_{20} \\ \bar{z}_{21} \\ \bar{z}_{22} \end{Bmatrix} = \underline{0} \quad (9)$$

$$\underline{B}_9(\omega) \begin{Bmatrix} \bar{z}_{23} \\ \bar{z}_{24} \\ \bar{z}_{25} \end{Bmatrix} = \underline{0} \quad (10)$$

$$\underline{B}_{10}(\omega) \begin{Bmatrix} \bar{z}_{26} \\ \bar{z}_{27} \\ \bar{z}_{28} \end{Bmatrix} = \underline{0} \quad (11)$$

$$\underline{B}_{11}(\omega) \begin{Bmatrix} \bar{z}_{29} \\ \bar{z}_{30} \end{Bmatrix} = \underline{0} \quad (12)$$

$$\underline{B}_{12}(\omega) \begin{Bmatrix} \underline{z}_{31} \\ \underline{z}_{32} \end{Bmatrix} = \underline{0} \quad (13)$$

The locations of the state vectors \underline{z}_i ($i = 1, 2, \dots, 32$) are shown in Fig. 2. The joint coupling matrices \underline{B}_i ($i = 1, 2, \dots, 12$) may be derived from the general formulas given in [3], or directly from first principles, as is done in Appendix A. The joint coupling matrices are written as a function of radian frequency ω because the elements of the joint coupling matrices depend, in general, on frequency. (Note, however, that for the rigid, massless joints considered here, the elements of the joint coupling matrices derived in Appendix A are independent of frequency.) The derivations of the joint coupling matrices in Appendix A are based on the assumption that each joint is completely unconstrained. Joint coupling matrices \underline{B}_1 , \underline{B}_2 , \underline{B}_{11} and \underline{B}_{12} are 6×12 matrices, and joint coupling matrices \underline{B}_3 through \underline{B}_{10} are 9×18 matrices. The right hand side of each of eqns. (2) through (13) is zero because it is assumed that there are no external forces or moments applied to the joints.

Eqns. (2) through (13) can be combined into a single equation of the form

$$\underline{B}_G(\omega) \underline{z}_G = \underline{0} \quad (14)$$

where \underline{B}_G is a global joint coupling matrix given by

$$\underline{B}_G(\omega) = \begin{bmatrix} \underline{B}_1 & \underline{0} & \cdot & \cdot & \cdot & \underline{0} \\ \underline{0} & \underline{B}_2 & & & & \cdot \\ \cdot & & \cdot & & & \cdot \\ \cdot & & & \cdot & & \cdot \\ \cdot & & & & \cdot & \underline{0} \\ \underline{0} & \cdot & \cdot & \cdot & \underline{0} & \underline{B}_{12} \end{bmatrix} \quad (15)$$

and $\underline{\bar{z}}_G$ is a global state vector given by

$$\underline{\bar{z}}_G = \left\{ \begin{array}{c} \underline{\bar{z}}_1 \\ \underline{\bar{z}}_2 \\ \cdot \\ \cdot \\ \cdot \\ \underline{\bar{z}}_{31} \\ \underline{\bar{z}}_{32} \end{array} \right\} \quad (16)$$

The global joint coupling matrix $\underline{B}_G(\omega)$ is a 96 x 192 matrix, and the global state vector $\underline{\bar{z}}_G$ is a 192 x 1 matrix. Eqn. (16) contains all the information about the dynamics of the joints in the lattice model of Fig. 2 and all the connectivity information (that is, information about which members are connected to which joints), but contains no information about the dynamics of the members of the lattice.

Transfer Matrix Relationships

The Fourier transforms $\underline{\bar{z}}_3$ and $\underline{\bar{z}}_1$ of the state vectors \underline{z}_3 and \underline{z}_1 in Fig. 2 are related by an equation of the form

$$\bar{z}_3 = \underline{T}(\omega)\bar{z}_1 \quad (17)$$

where $\underline{T}(\omega)$ is the 6 x 6 transfer matrix of the member connecting joints 1 and 2. Eqn. (17) is the transfer matrix relationship for the member connecting joints 1 and 2. The transfer matrix for the Bernoulli-Euler beam model and the transfer matrix for the Timoshenko beam model are given in Appendix B. The transfer matrix is written as a function of radian frequency ω because the elements of \underline{T} depend, in general, on frequency. Transfer matrix relationships for each of the remaining members in the lattice model of Fig. 2 can be written as

$$\bar{z}_5 = \underline{T}(\omega)\bar{z}_2 \quad (18)$$

$$\bar{z}_9 = \underline{T}(\omega)\bar{z}_4 \quad (19)$$

$$\bar{z}_8 = \underline{T}(\omega)\bar{z}_7 \quad (20)$$

$$\bar{z}_{11} = \underline{T}(\omega)\bar{z}_6 \quad (21)$$

$$\bar{z}_{15} = \underline{T}(\omega)\bar{z}_{10} \quad (22)$$

$$\bar{z}_{14} = \underline{T}(\omega)\bar{z}_{13} \quad (23)$$

$$\bar{z}_{17} = \underline{T}(\omega)\bar{z}_{12} \quad (24)$$

$$\bar{z}_{21} = \underline{T}(\omega)\bar{z}_{16} \quad (25)$$

$$\bar{z}_{20} = \underline{T}(\omega)\bar{z}_{19} \quad (26)$$

$$\bar{z}_{23} = \underline{T}(\omega)\bar{z}_{18} \quad (27)$$

$$\bar{z}_{27} = \underline{T}(\omega)\bar{z}_{22} \quad (28)$$

$$\bar{z}_{26} = \underline{T}(\omega)\bar{z}_{25} \quad (29)$$

$$\bar{z}_{29} = \underline{T}(\omega)\bar{z}_{24} \quad (30)$$

$$\bar{z}_{32} = \underline{T}(\omega)\bar{z}_{28} \quad (31)$$

$$\bar{z}_{31} = \underline{T}(\omega)\bar{z}_{30} \quad (32)$$

The transfer matrices in eqns. (17) through (32) are identical because the members in Fig. 2 are identical, and because of the choice of the local coordinate directions. (As discussed in [1], reversing the sense of the local coordinate direction changes the transfer matrix.)

Eqns. (17) through (30) can be combined into a single equation of the form

$$\bar{z}_{-G} = \underline{T}_{-G}(\omega)\bar{z}_{-G/2} \quad (33)$$

where the global state vector \bar{z}_{-G} is given by eqn. (16), $\underline{T}_{-G}(\omega)$ is a 92 x 196 global transfer matrix given by

and $\bar{z}_{G/2}$ is a 96 row vector given by

$$\bar{z}_{G/2} = \left\{ \begin{array}{l} \bar{z}_1 \\ \bar{z}_2 \\ \bar{z}_4 \\ \bar{z}_6 \\ \bar{z}_7 \\ \bar{z}_{10} \\ \bar{z}_{12} \\ \bar{z}_{13} \\ \bar{z}_{16} \\ \bar{z}_{18} \\ \bar{z}_{19} \\ \bar{z}_{22} \\ \bar{z}_{24} \\ \bar{z}_{25} \\ \bar{z}_{28} \\ \bar{z}_{30} \end{array} \right\} \quad (35)$$

The matrix \underline{I} in eqn. (34) is the 6 x 6 identity matrix. The vector $\bar{z}_{G/2}$ contains half the state vectors in \bar{z}_G . Eqn. (35) contains all the information about the dynamics of the members in the lattice model of Fig. 2, but contains no information about the joint dynamics and no connectivity information.

Determination of Natural Frequencies

Substitution of eqn. (33) into eqn. (14) gives

$$\underline{B}_G(\omega)\underline{T}_G(\omega)\bar{\underline{Z}}_{G/2} = \underline{0} \quad (36)$$

where the product $\underline{B}_G(\omega)\underline{T}_G(\omega)$ is a 96 x 96 matrix. For each value of ω , eqn. (36) is a system of homogeneous linear equations for the components of the state vector $\bar{\underline{Z}}_{G/2}$. The values of ω for which a nontrivial solution for $\bar{\underline{Z}}_{G/2}$ may exist must satisfy the equation

$$\det(\underline{B}_G(\omega)\underline{T}_G(\omega)) = 0 \quad (37)$$

The values of ω which satisfy eqn. (37) are the natural frequencies of the lattice model of Fig. 2.

Because the global transfer matrix \underline{T}_G contains trigonometric and hyperbolic functions of ω , eqn. (37) is a nonlinear transcendental equation in ω . Since the members of the lattice model of Fig. 2 are modeled as continuous beams, there is an infinite number of values of ω which satisfy eqn. (37).

NUMERICAL RESULTS

Method of Computation

In order to solve eqn. (37) for ω , the determinant of $\underline{B}_G(\omega)\underline{T}_G(\omega)$ can be plotted numerically as a function of ω , and the values of ω for which the determinant equals zero can be determined graphically. Alternatively, a root-finding algorithm such as the bisection method or the secant method [7] can be used.

Both the graphical method and the root-finding algorithms require a numerical evaluation of $\det(\underline{B}_G(\omega)\underline{T}_G(\omega))$. Since most of the elements of $\underline{B}_G(\omega)$ and $\underline{T}_G(\omega)$ are zero, it is very inefficient to encode $\underline{B}_G(\omega)$ and $\underline{T}_G(\omega)$ into a computer program directly from eqns. (15) and (34). The matrices $\underline{B}_G(\omega)$ and $\underline{T}_G(\omega)$ are simple enough that the product $\underline{B}_G(\omega)\underline{T}_G(\omega)$ may be computed in 6 x 6 block form by hand. The result of such a hand computation shows that $\underline{B}_G(\omega)\underline{T}_G(\omega)$ is a banded matrix. Thus the determinant of $\underline{B}_G(\omega)\underline{T}_G(\omega)$ may be computed efficiently by using a computer algorithm specifically designed for banded matrices.

The PASCAL language computer program used here to evaluate $\det(\underline{B}_G(\omega)\underline{T}_G(\omega))$ as a function of ω is listed in Appendix C. The heart of the program is the procedure bandet, which is based on a Gaussian elimination algorithm designed to solve a system of linear equations with a banded coefficient matrix. A discussion of this Gaussian elimination algorithm is given in [8]. Only the portions of the bandet procedure given in [8] which are necessary to evaluate the determinant of the banded matrix are used here.

Numerical results for the first twenty-five nonzero natural frequencies of the lattice model for the case when the lattice members are modeled as Bernoulli-Euler beams and for the case when the lattice members are modeled

as Timoshenko beams are given in Table 1. The results in Table 1 are obtained by first plotting $\det(\underline{B}_G(\omega)\underline{T}_G(\omega))$ as a function of ω in steps of 10 rad/sec to evaluate the approximate location of the zero crossings, and then evaluating $\det(\underline{B}_G(\omega)\underline{T}_G(\omega))$ as a function of ω in steps of 1 rad/sec in the neighborhood of a zero crossing. The value of the natural frequency is then taken as the average of the two values between which $\det(\underline{B}_G(\omega)\underline{T}_G(\omega))$ changes sign. The material and geometric properties of the lattice members which are used in the computations are given in Appendix B. A typical plot of $\det(\underline{B}_G(\omega)\underline{T}_G(\omega))$ as a function of ω is shown in Fig. 4. The square data points represent the values of $\det(\underline{B}_G(\omega)\underline{T}_G(\omega))$ which were actually computed, and the curve is a smooth (second order polynomial) fit to the data points.

An interesting section of the function $\det(\underline{B}_G(\omega)\underline{T}_G(\omega))$ is shown in Fig. 5. It appears from Fig. 5 that $\det(\underline{B}_G(\omega)\underline{T}_G(\omega))$ takes the value zero somewhere near $\omega = 3250$ rad/sec. The very small slope near $\omega = 3250$ rad/sec suggests that the zero near $\omega = 3250$ rad/sec may be a multiple zero. (A multiple zero of multiplicity k is a value of ω for which $\det(\underline{B}_G(\omega)\underline{T}_G(\omega)) = 0$ and the first $k-1$ derivatives of $\det(\underline{B}_G(\omega)\underline{T}_G(\omega))$ with respect to ω are also equal to zero.) However, an evaluation of $\det(\underline{B}_G(\omega)\underline{T}_G(\omega))$ near $\omega = 3250$ rad/sec with a smaller step size for ω (see Fig. 6) shows that there are in fact five distinct zero crossings between $\omega = 3242$ rad/sec and $\omega = 3260$ rad/sec. (Note that the vertical scale of Fig. 6 is much different from the vertical scale of Fig. 5.)

The natural frequencies computed with the Bernoulli-Euler beam lattice model are plotted as a function of flexible mode number in Fig. 7. Fig. 7 also shows the natural frequencies obtained in a previous analysis [6] using a finite element method and an experimental modal analysis. It is seen

that excellent agreement is obtained between the natural frequencies computed here and those given in [6]. The maximum difference between the results obtained here and those given in [6] is six percent.

DISCUSSION

The number of natural frequencies in Table 1 was chosen arbitrarily. The method presented here can be used to compute as many natural frequencies as desired. For large ω , the value of $\det(\underline{B}_G(\omega)\underline{T}_G(\omega))$ may be larger than the largest number which a particular computer can store, but this problem may be overcome by introducing scale factors into the calculation of the determinant [8]. As shown by the discussion concerning Figs. 5 and 6, some care is required in finding the natural frequencies, since they may be very closely spaced in some frequency ranges.

The results in Table 1 show that rotary inertia and shear deformation of the lattice members, which the Timoshenko beam model includes and which the Bernoulli-Euler beam model does not, have very little effect on the natural frequencies of the lattice model for the frequency range considered here. Note, however, that the natural frequencies predicted by the Timoshenko beam model are less than or equal to the frequencies predicted by the Bernoulli-Euler beam model, and that the difference between the two models increases with increasing frequency. It can be shown analytically that for a single beam which is simply supported at each end, the effect of rotary inertia and shear deformation is to decrease the natural frequencies of flexural vibration, and that the effect increases with increasing frequency [9].

The joint models adopted here are perhaps the simplest possible. However, the excellent agreement between the results computed here and the results of the experimental analysis in [6] shows that the simple joint models are certainly useful in the frequency range considered here. Also, more complicated joint models may be included in the present analysis with

only minor difficulties; all that is needed is a joint coupling matrix for each joint. Joint coupling matrices for two and three-dimensional rigid joints with arbitrary mass and arbitrary spatial dimensions are derived in [3].

CONCLUSIONS AND RECOMMENDATIONS

The type of analysis presented here may be applied to any system which may be modeled as a connected network of one-dimensional members. (Note, for example, that this kind of analysis is not restricted to structural or mechanical systems, and is related to techniques used in the analysis of electrical and microwave networks [10].) The necessary numerical computations are straightforward, and are easily performed with a personal computer.

As discussed above, the effect of various member models and joint models on the natural frequencies of the lattice may be determined by simply altering the appropriate transfer matrices and joint coupling matrices. Also, and perhaps more importantly, the effects of changes in the structure of the lattice may be considered using the techniques presented here. Changes in structure may be due, for example, to disconnected joints or damaged members. Thus the techniques discussed here may be used to begin to study the following nondestructive evaluation question: given a measurement of, say, certain natural frequencies of a lattice structure, what is it possible to conclude about the structural integrity of the lattice? This nondestructive evaluation question may also be expressed in the wider context of the system identification problem, in which the properties of an unknown system are deduced from certain measurements of the system.

REFERENCES

- [1] J.H. Williams, Jr., F.C. Eng and S.S. Lee, "Wave Propagation and Dynamics of Lattice Structures", AFOSR Technical Report, May 1984.
- [2] A. Von Flotow, "Disturbance Propagation in Structural Networks; Control of Large Space Structures", Ph.D. Thesis, Stanford University, Palo Alto, CA, June 1984.
- [3] J.H. Williams, Jr., H.K. Yeung and R.J. Nagem, "Joint Coupling Matrices for Wave Propagation Analysis of Large Space Structures", AFOSR Technical Report, July 1986.
- [4] J.H. Williams, Jr., R.J. Nagem and H.K. Yeung, "Wave-Mode Coordinates and Scattering Matrices for Dynamic Analysis of Large Space Structures", AFOSR Technical Report, October 1986.
- [5] J.H. Williams, Jr., R.J. Nagem and H.K. Yeung, "Pulse Propagation in a One-Dimensional Lattice Structure: A Comparison of the Pulse Summation Method and the Wave-Mode Coordinate Method", AFOSR Technical Report, December 1986.
- [6] J.H. Williams, Jr., R.A. Schroeder and S.S. Lee, "Dynamic Analyses of Two-Dimensional Lattices", AFOSR Technical Report, August 1984.
- [7] S.D. Conte and C. deBoor, Elementary Numerical Analysis: An Algorithmic Approach, McGraw-Hill, 1972.
- [8] J.H. Wilkinson and C. Reinsch, Linear Algebra, Springer-Verlag, 1971.
- [9] S. Timoshenko, Vibration Problems in Engineering, D. Van Nostrand, 1955.
- [10] R.W. Newcomb, Linear Multiport Synthesis, McGraw-Hill, 1960.
- [11] E.C. Pestel and F.A. Leckie, Matrix Methods in Elastomechanics, McGraw-Hill, 1963.

TABLE 1 First twenty-five nonzero natural frequencies of lattice model.

Flexible Mode Number	Bernoulli-Euler Beams (rad/sec)	Timoshenko Beams (rad/sec)
1	308.5	308.5
2	433.5	433.5
3	606.5	605.5
4	726.5	725.5
5	932.5	931.5
6	1438.5	1437.5
7	1535.5	1534.5
8	1766.5	1764.5
9	2071.5	2067.5
10	2115.5	2111.5
11	2307.5	2303.5
12	2479.5	2474.5
13	2887.5	2881.5
14	2979.5	2973.5
15	3242.5	3232.5
16	3249.5	3238.5
17	3254.5	3243.5
18	3257.5	3246.5
19	3258.5	3248.5
20	3552.5	3544.5
21	4120.5	4108.5
22	5923.5	5903.5
23	6094.5	6072.5
24	6704.5	6675.5
25	6894.5	6861.5

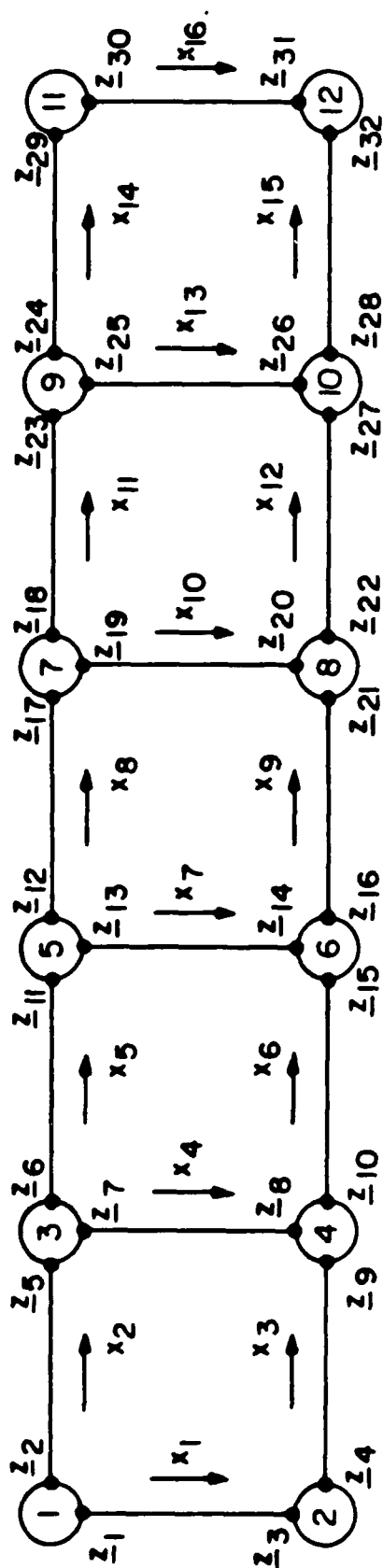


Fig. 2 Lattice model.

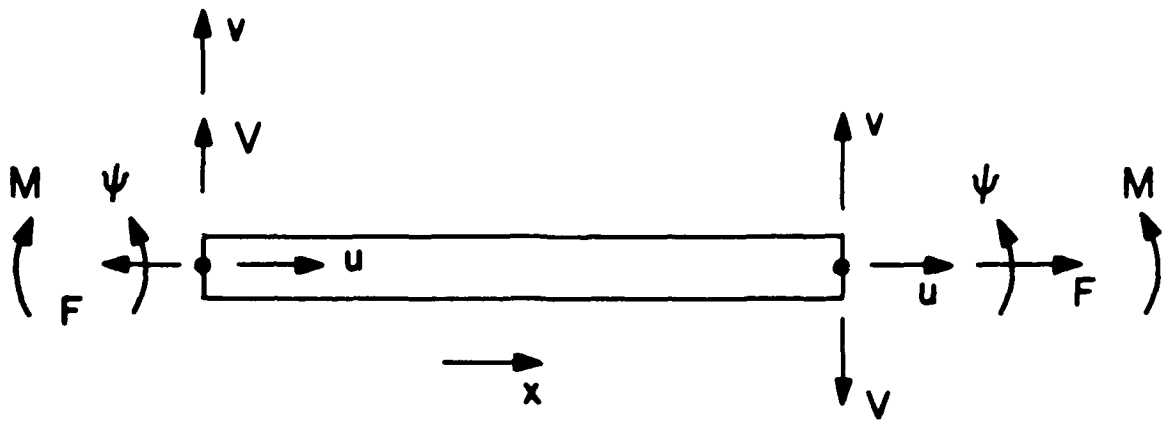


Fig. 3 Lattice member, showing components of state vectors and sign convention.

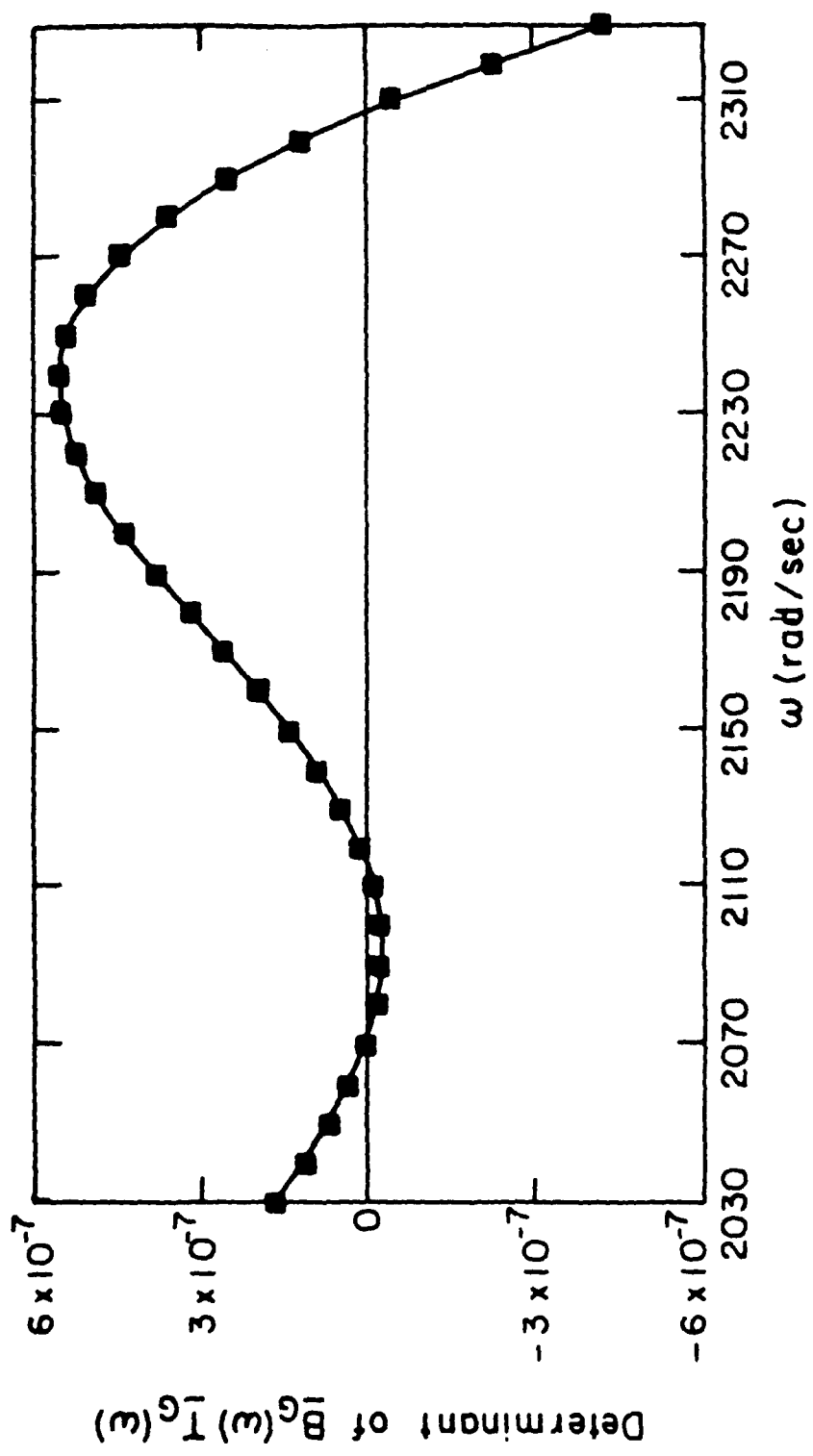


Fig. 4 Typical plot of $\det(B_G(\omega) T_G(\omega))$ as a function of ω , obtained using Bernoulli-Euler beam model.

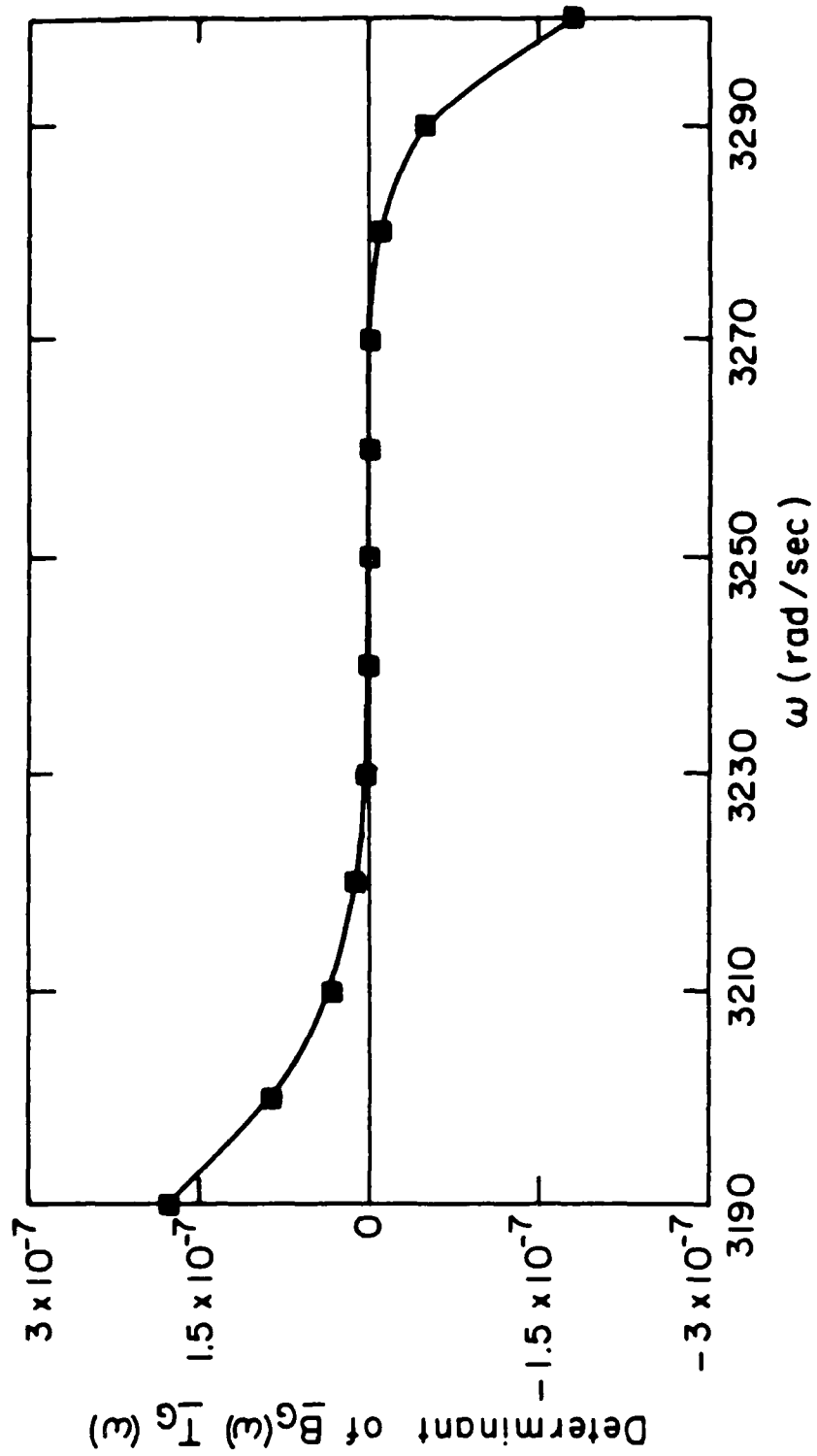


Fig. 5 Plot of $\det(B_G(\omega) T_G(\omega))$ as a function of ω , obtained using Bernoulli-Euler beam model.

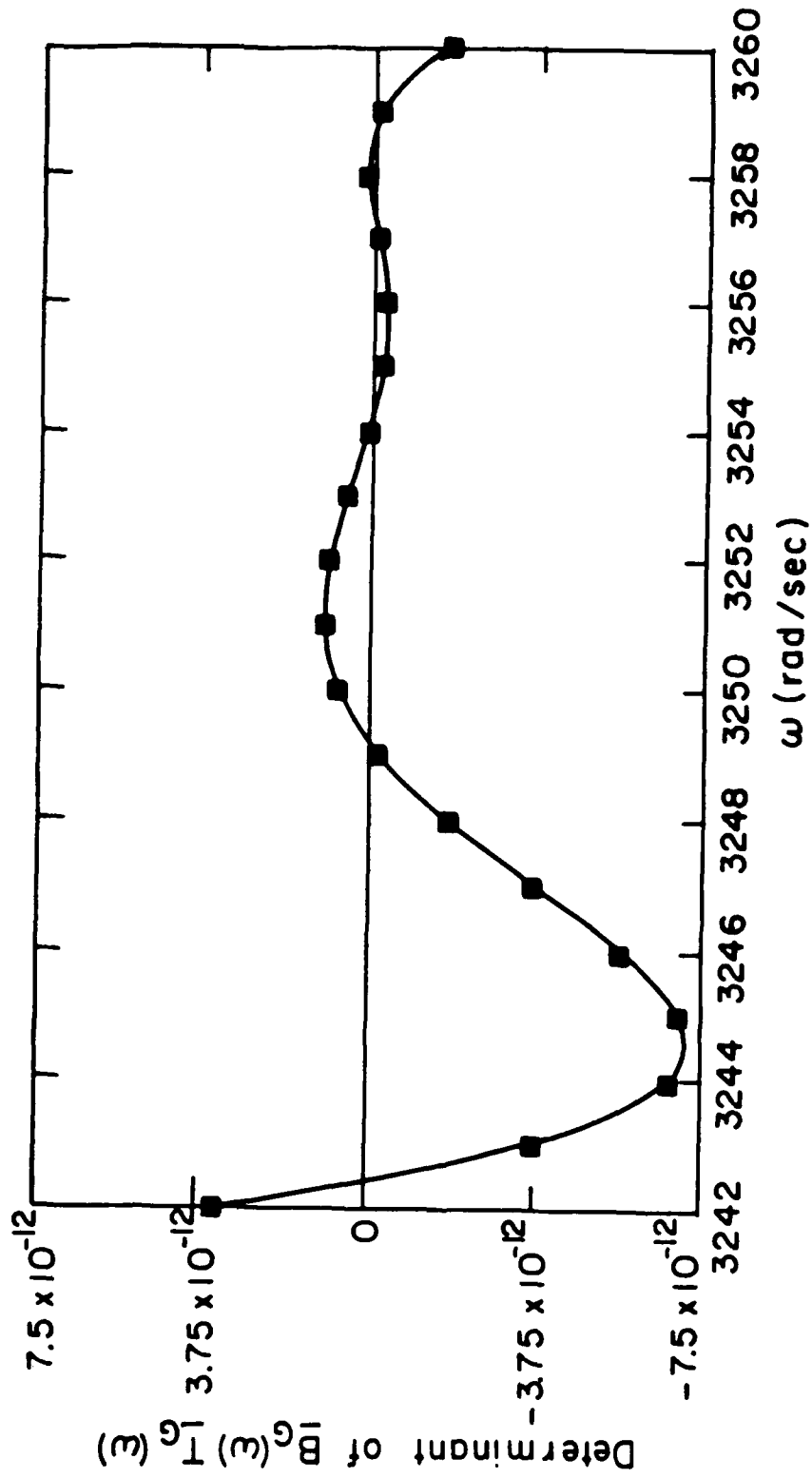


Fig. 6 Expanded plot of $\det(B_G(\omega) T_G(\omega))$ as a function of ω near $\omega = 3250$ rad/sec, obtained using Bernoulli-Euler beam model.

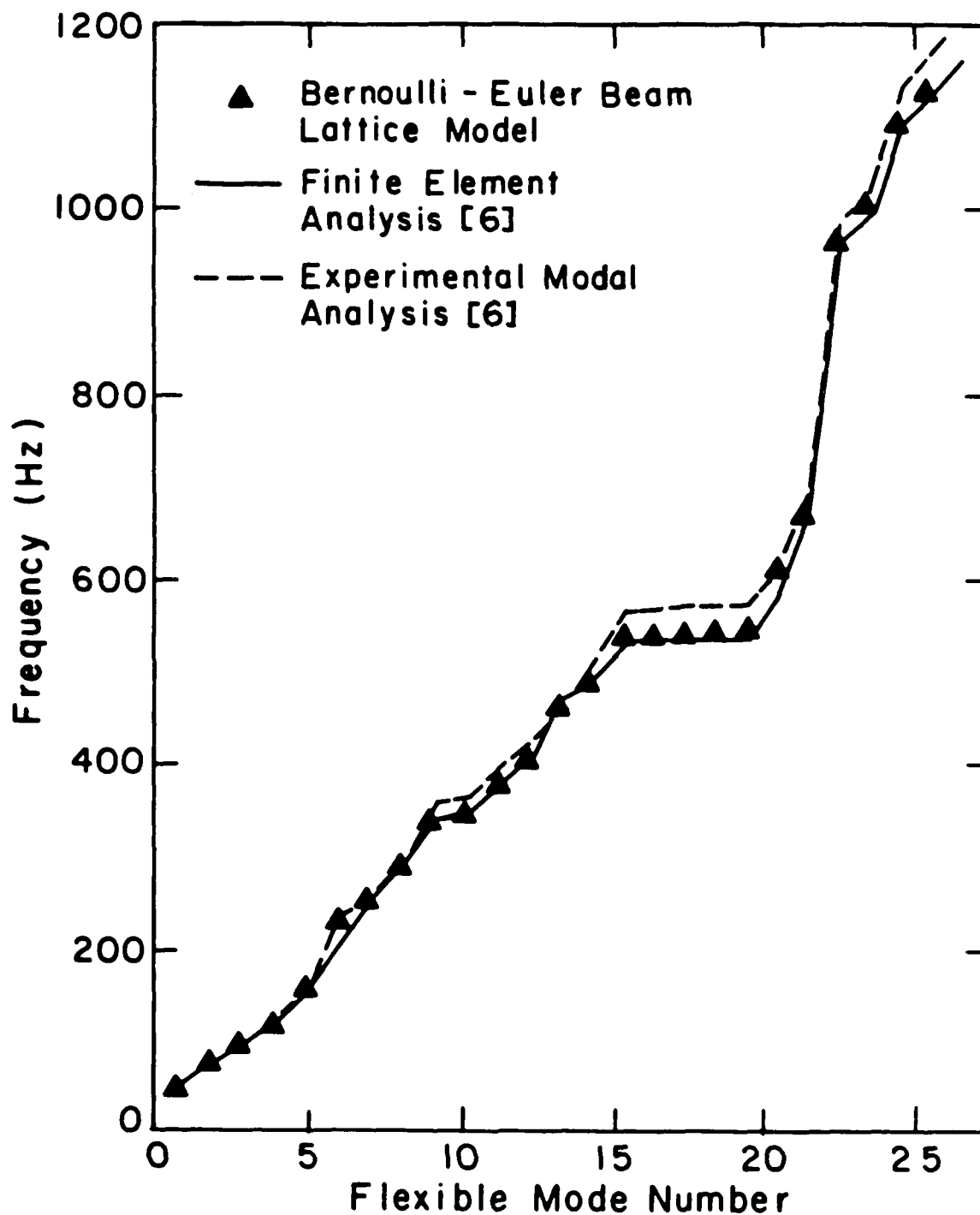


Fig. 7 Natural frequencies obtained by finite element analysis, experimental modal analysis, and Bernoulli-Euler beam lattice model.

APPENDIX A: DERIVATION OF JOINT COUPLING MATRICES

In this appendix, the joint coupling matrices for the lattice model of Fig. A1 are derived. The joints of the lattice model are labeled 1 through 12 as shown in Fig. A1. It is assumed that all joints and members can move only in the plane of the lattice, and that all motions are small. It is also assumed that each joint is rigid, massless, and has no spatial extent, and that each connection between a member and a joint is rigid.

The state vector at any point x of any member of the lattice model of Fig. A1 is assumed to be of the form

$$\underline{z}(x,t) = \begin{Bmatrix} u(x,t) \\ v(x,t) \\ \psi(x,t) \\ M(x,t) \\ V(x,t) \\ F(x,t) \end{Bmatrix} \quad (A1)$$

where $u(x,t)$ is the longitudinal displacement of the member, $v(x,t)$ is the transverse displacement of the member, $\psi(x,t)$ is the rotation of the member, $M(x,t)$ is the bending moment in the member, $V(x,t)$ is the shear force in the member, $F(x,t)$ is the axial force in the member, x is a spatial coordinate which extends along the length of the member and t is time. The components of the state vector and the sign convention adopted here for the components of the state vector are shown in Fig. A2. Local coordinate directions x_i ($i = 1, 2, \dots, 16$) are assigned to the lattice members as shown in Fig. A1. Throughout this appendix, an overbar will denote a Fourier transform.

Joint 1

The components of the state vectors \underline{z}_1 and \underline{z}_2 and a free-body diagram of joint 1 are shown in Fig. A3. The equilibrium equations for joint 1 are

$$M_1 + M_2 = 0 \quad (A2)$$

$$V_1 - F_2 = 0 \quad (A3)$$

$$F_1 + V_2 = 0 \quad (A4)$$

Eqns. (A2), (A3) and (A4) can be written in matrix form as

$$\begin{bmatrix} 1 & 0 & 0 \\ 0 & 1 & 0 \\ 0 & 0 & 1 \end{bmatrix} \begin{Bmatrix} M_1 \\ V_1 \\ F_1 \end{Bmatrix} + \begin{bmatrix} 1 & 0 & 0 \\ 0 & 0 & -1 \\ 0 & 1 & 0 \end{bmatrix} \begin{Bmatrix} M_2 \\ V_2 \\ F_2 \end{Bmatrix} = \begin{Bmatrix} 0 \\ 0 \\ 0 \end{Bmatrix} \quad (A5)$$

The compatibility equations for joint 1 are

$$u_1 + v_2 = 0 \quad (A6)$$

$$v_1 - u_2 = 0 \quad (A7)$$

$$\psi_1 - \psi_2 = 0 \quad (A8)$$

Eqns. (A6), (A7) and (A8) can be written in matrix form as

$$\begin{bmatrix} 1 & 0 & 0 \\ 0 & 1 & 0 \\ 0 & 0 & 1 \end{bmatrix} \begin{Bmatrix} u_1 \\ v_1 \\ \psi_1 \end{Bmatrix} + \begin{bmatrix} 0 & 1 & 0 \\ -1 & 0 & 0 \\ 0 & 0 & -1 \end{bmatrix} \begin{Bmatrix} u_2 \\ v_2 \\ \psi_2 \end{Bmatrix} = \begin{Bmatrix} 0 \\ 0 \\ 0 \end{Bmatrix} \quad (A9)$$

Combining eqns. (A5) and (A9) and taking the Fourier transform of the resulting equation give

$$\begin{bmatrix}
 1 & 0 & 0 & 0 & 0 & 0 & 0 & 1 & 0 & 0 & 0 & 0 \\
 0 & 1 & 0 & 0 & 0 & 0 & -1 & 0 & 0 & 0 & 0 & 0 \\
 0 & 0 & 1 & 0 & 0 & 0 & 0 & 0 & -1 & 0 & 0 & 0 \\
 0 & 0 & 0 & 1 & 0 & 0 & 0 & 0 & 0 & 1 & 0 & 0 \\
 0 & 0 & 0 & 0 & 1 & 0 & 0 & 0 & 0 & 0 & 0 & -1 \\
 0 & 0 & 0 & 0 & 0 & 1 & 0 & 0 & 0 & 0 & 1 & 0
 \end{bmatrix}
 \begin{Bmatrix}
 \bar{u}_1 \\
 \bar{v}_1 \\
 \bar{r}_1 \\
 \bar{M}_1 \\
 \bar{v}_1 \\
 \bar{F}_1 \\
 \bar{u}_2 \\
 \bar{v}_2 \\
 \bar{\psi}_2 \\
 \bar{M}_2 \\
 \bar{v}_2 \\
 \bar{F}_2
 \end{Bmatrix}
 =
 \begin{Bmatrix}
 0 \\
 0 \\
 0 \\
 0 \\
 0 \\
 0 \\
 0 \\
 0 \\
 0 \\
 0 \\
 0 \\
 0
 \end{Bmatrix}
 \quad (A10)$$

The 6 x 12 matrix in eqn. (A10) is the joint coupling matrix \underline{B}_1 of joint 1.

Joint 2

The components of the state vectors \underline{z}_3 and \underline{z}_4 and a free-body diagram of joint 2 are shown in Fig. A4. The equilibrium equations for joint 2 are

$$\begin{bmatrix}
 1 & 0 & 0 \\
 0 & 1 & 0 \\
 0 & 0 & 1
 \end{bmatrix}
 \begin{Bmatrix}
 M_3 \\
 V_3 \\
 F_3
 \end{Bmatrix}
 +
 \begin{bmatrix}
 -1 & 0 & 0 \\
 0 & 0 & 1 \\
 0 & -1 & 0
 \end{bmatrix}
 \begin{Bmatrix}
 M_4 \\
 V_4 \\
 F_4
 \end{Bmatrix}
 =
 \begin{Bmatrix}
 0 \\
 0 \\
 0
 \end{Bmatrix}
 \quad (A11)$$

The compatibility equations for joint 2 are

$$\begin{bmatrix} 1 & 0 & 0 \\ 0 & 1 & 0 \\ 0 & 0 & 1 \end{bmatrix} \begin{Bmatrix} u_3 \\ v_3 \\ \psi_3 \end{Bmatrix} + \begin{bmatrix} 0 & 1 & 0 \\ -1 & 0 & 0 \\ 0 & 0 & -1 \end{bmatrix} \begin{Bmatrix} u_4 \\ v_4 \\ \psi_4 \end{Bmatrix} = \begin{Bmatrix} 0 \\ 0 \\ 0 \end{Bmatrix} \quad (\text{A12})$$

Combining eqns. (A11) and (A12) and taking the Fourier transform of the resulting equation give

$$\begin{bmatrix} 1 & 0 & 0 & 0 & 0 & 0 & 0 & 1 & 0 & 0 & 0 & 0 \\ 0 & 1 & 0 & 0 & 0 & 0 & -1 & 0 & 0 & 0 & 0 & 0 \\ 0 & 0 & 1 & 0 & 0 & 0 & 0 & 0 & -1 & 0 & 0 & 0 \\ 0 & 0 & 0 & 1 & 0 & 0 & 0 & 0 & 0 & -1 & 0 & 0 \\ 0 & 0 & 0 & 0 & 1 & 0 & 0 & 0 & 0 & 0 & 0 & 1 \\ 0 & 0 & 0 & 0 & 0 & 1 & 0 & 0 & 0 & 0 & -1 & 0 \end{bmatrix} \begin{Bmatrix} \bar{u}_3 \\ \bar{v}_3 \\ \bar{\psi}_3 \\ \bar{M}_3 \\ \bar{V}_3 \\ \bar{F}_3 \\ \bar{u}_4 \\ \bar{v}_4 \\ \bar{\psi}_4 \\ \bar{M}_4 \\ \bar{V}_4 \\ \bar{F}_4 \end{Bmatrix} = \begin{Bmatrix} 0 \\ 0 \\ 0 \\ 0 \\ 0 \\ 0 \end{Bmatrix} \quad (\text{A13})$$

The 6 x 12 matrix in eqn. (A13) is the joint coupling matrix \underline{B}_2 of joint 2.

Joint 3

The components of the state vectors \underline{z}_5 , \underline{z}_6 and \underline{z}_7 and a free-body diagram of joint 3 are shown in Fig. A5. The equilibrium equations for joint 3 are

$$M_5 - M_6 - M_7 = 0 \quad (A14)$$

$$V_5 - V_6 - F_7 = 0 \quad (A15)$$

$$F_5 - F_6 + V_7 = 0 \quad (A16)$$

Eqns. (A14), (A15) and (A16) can be written in matrix form as

$$\begin{bmatrix} 1 & 0 & 0 \\ 0 & 1 & 0 \\ 0 & 0 & 1 \end{bmatrix} \begin{Bmatrix} M_5 \\ V_5 \\ F_5 \end{Bmatrix} + \begin{bmatrix} -1 & 0 & 0 \\ 0 & -1 & 0 \\ 0 & 0 & -1 \end{bmatrix} \begin{Bmatrix} M_6 \\ V_6 \\ F_6 \end{Bmatrix} + \begin{bmatrix} -1 & 0 & 0 \\ 0 & 0 & -1 \\ 0 & 1 & 0 \end{bmatrix} \begin{Bmatrix} M_7 \\ V_7 \\ F_7 \end{Bmatrix} = \begin{Bmatrix} 0 \\ 0 \\ 0 \end{Bmatrix} \quad (A17)$$

The compatibility equations for joint 3 are

$$u_5 - u_6 = 0 \quad (A18)$$

$$v_5 - v_6 = 0 \quad (A19)$$

$$\psi_5 - \psi_6 = 0 \quad (A20)$$

$$u_5 - v_7 = 0 \quad (A21)$$

$$v_5 + u_7 = 0 \quad (A22)$$

$$\psi_5 - \psi_7 = 0 \quad (A23)$$

Eqns. (A18) through (A23) can be written in matrix form as

$$\begin{bmatrix} 1 & 0 & 0 \\ 0 & 1 & 0 \\ 0 & 0 & 1 \end{bmatrix} \begin{Bmatrix} u_5 \\ v_5 \\ r_5 \end{Bmatrix} + \begin{bmatrix} -1 & 0 & 0 \\ 0 & -1 & 0 \\ 0 & 0 & -1 \end{bmatrix} \begin{Bmatrix} u_6 \\ v_6 \\ r_6 \end{Bmatrix} = \begin{Bmatrix} 0 \\ 0 \\ 0 \end{Bmatrix} \quad (\text{A24})$$

and

$$\begin{bmatrix} 1 & 0 & 0 \\ 0 & 1 & 0 \\ 0 & 0 & 1 \end{bmatrix} \begin{Bmatrix} u_5 \\ v_5 \\ r_5 \end{Bmatrix} + \begin{bmatrix} 0 & -1 & 0 \\ 1 & 0 & 0 \\ 0 & 0 & -1 \end{bmatrix} \begin{Bmatrix} u_7 \\ v_7 \\ r_7 \end{Bmatrix} = \begin{Bmatrix} 0 \\ 0 \\ 0 \end{Bmatrix} \quad (\text{A25})$$

Combining eqns. (A17), (A24) and (A25) and taking the Fourier of the resulting equation give

$$\begin{bmatrix}
 1 & 0 & 0 & 0 & 0 & 0 & -1 & 0 & 0 & 0 & 0 & 0 & 0 & 0 & 0 & 0 & 0 \\
 0 & 1 & 0 & 0 & 0 & 0 & 0 & -1 & 0 & 0 & 0 & 0 & 0 & 0 & 0 & 0 & 0 \\
 0 & 0 & 1 & 0 & 0 & 0 & 0 & 0 & -1 & 0 & 0 & 0 & 0 & 0 & 0 & 0 & 0 \\
 1 & 0 & 0 & 0 & 0 & 0 & 0 & 0 & 0 & 0 & 0 & 0 & 0 & -1 & 0 & 0 & 0 \\
 0 & 1 & 0 & 0 & 0 & 0 & 0 & 0 & 0 & 0 & 0 & 0 & 0 & 1 & 0 & 0 & 0 \\
 0 & 0 & 1 & 0 & 0 & 0 & 0 & 0 & 0 & 0 & 0 & 0 & 0 & 0 & -1 & 0 & 0 \\
 0 & 0 & 0 & 1 & 0 & 0 & 0 & 0 & -1 & 0 & 0 & 0 & 0 & 0 & -1 & 0 & 0 \\
 0 & 0 & 0 & 0 & 1 & 0 & 0 & 0 & 0 & -1 & 0 & 0 & 0 & 0 & 0 & 0 & -1 \\
 0 & 0 & 0 & 0 & 0 & 1 & 0 & 0 & 0 & 0 & -1 & 0 & 0 & 0 & 0 & 1 & 0
 \end{bmatrix}
 \begin{Bmatrix}
 \bar{u}_5 \\
 \bar{v}_5 \\
 \bar{\psi}_5 \\
 \bar{M}_5 \\
 \bar{V}_5 \\
 \bar{F}_5 \\
 \bar{u}_6 \\
 \bar{v}_6 \\
 \bar{\psi}_6 \\
 \bar{M}_6 \\
 \bar{V}_6 \\
 \bar{F}_6 \\
 \bar{u}_7 \\
 \bar{v}_7 \\
 \bar{\psi}_7 \\
 \bar{M}_7 \\
 \bar{V}_7 \\
 \bar{F}_7
 \end{Bmatrix}
 =
 \begin{Bmatrix}
 0 \\
 0 \\
 0 \\
 0 \\
 0 \\
 0 \\
 0 \\
 0 \\
 0 \\
 0 \\
 0 \\
 0 \\
 0 \\
 0 \\
 0 \\
 0 \\
 0
 \end{Bmatrix}
 \quad (A26)$$

The 9×18 matrix in eqn. (A26) is the joint coupling matrix \underline{B}_3 of joint 3.

Joint 4

The components of the state vectors \underline{z}_8 , \underline{z}_9 and \underline{z}_{10} and a free-body diagram of joint 4 are shown in Fig. A6. The equilibrium equations for joint 4 are

$$\begin{bmatrix} 1 & 0 & 0 \\ 0 & 1 & 0 \\ 0 & 0 & 1 \end{bmatrix} \begin{Bmatrix} M_8 \\ V_8 \\ F_8 \end{Bmatrix} + \begin{bmatrix} 1 & 0 & 0 \\ 0 & 0 & -1 \\ 0 & 1 & 0 \end{bmatrix} \begin{Bmatrix} M_9 \\ V_9 \\ F_9 \end{Bmatrix} + \begin{bmatrix} -1 & 0 & 0 \\ 0 & 0 & 1 \\ 0 & -1 & 0 \end{bmatrix} \begin{Bmatrix} M_{10} \\ V_{10} \\ F_{10} \end{Bmatrix} = \begin{Bmatrix} 0 \\ 0 \\ 0 \end{Bmatrix} \quad (\text{A27})$$

The compatibility equations for joint 4 are

$$\begin{bmatrix} 1 & 0 & 0 \\ 0 & 1 & 0 \\ 0 & 0 & 1 \end{bmatrix} \begin{Bmatrix} u_8 \\ v_8 \\ \psi_8 \end{Bmatrix} + \begin{bmatrix} 0 & 1 & 0 \\ -1 & 0 & 0 \\ 0 & 0 & -1 \end{bmatrix} \begin{Bmatrix} u_9 \\ v_9 \\ \psi_9 \end{Bmatrix} = \begin{Bmatrix} 0 \\ 0 \\ 0 \end{Bmatrix} \quad (\text{A28})$$

$$\begin{bmatrix} 1 & 0 & 0 \\ 0 & 1 & 0 \\ 0 & 0 & 1 \end{bmatrix} \begin{Bmatrix} u_8 \\ v_8 \\ \psi_8 \end{Bmatrix} + \begin{bmatrix} 0 & 1 & 0 \\ -1 & 0 & 0 \\ 0 & 0 & -1 \end{bmatrix} \begin{Bmatrix} u_{10} \\ v_{10} \\ \psi_{10} \end{Bmatrix} = \begin{Bmatrix} 0 \\ 0 \\ 0 \end{Bmatrix} \quad (\text{A29})$$

Combining eqns. (A27), (A28) and (A29) and taking the Fourier transform of the resulting equation give

$$\begin{bmatrix}
 1 & 0 & 0 & 0 & 0 & 0 & 0 & 1 & 0 & 0 & 0 & 0 & 0 & 0 & 0 & 0 & 0 \\
 0 & 1 & 0 & 0 & 0 & 0 & -1 & 0 & 0 & 0 & 0 & 0 & 0 & 0 & 0 & 0 & 0 \\
 0 & 0 & 1 & 0 & 0 & 0 & 0 & 0 & -1 & 0 & 0 & 0 & 0 & 0 & 0 & 0 & 0 \\
 1 & 0 & 0 & 0 & 0 & 0 & 0 & 0 & 0 & 0 & 0 & 0 & 0 & 1 & 0 & 0 & 0 \\
 0 & 1 & 0 & 0 & 0 & 0 & 0 & 0 & 0 & 0 & 0 & 0 & -1 & 0 & 0 & 0 & 0 \\
 0 & 0 & 1 & 0 & 0 & 0 & 0 & 0 & 0 & 0 & 0 & 0 & 0 & 0 & -1 & 0 & 0 \\
 0 & 0 & 0 & 1 & 0 & 0 & 0 & 0 & 0 & 1 & 0 & 0 & 0 & 0 & 0 & -1 & 0 \\
 0 & 0 & 0 & 0 & 1 & 0 & 0 & 0 & 0 & 0 & 0 & -1 & 0 & 0 & 0 & 0 & 1 \\
 0 & 0 & 0 & 0 & 0 & 1 & 0 & 0 & 0 & 0 & 1 & 0 & 0 & 0 & 0 & 0 & -1
 \end{bmatrix}$$

$$\left. \begin{array}{c}
 \left. \begin{array}{c} \bar{u}_8 \\ \bar{v}_8 \\ \bar{\psi}_8 \\ \bar{M}_8 \\ \bar{V}_8 \\ \bar{F}_8 \end{array} \right\} \\
 \left. \begin{array}{c} \bar{u}_9 \\ \bar{v}_9 \\ \bar{\psi}_9 \\ \bar{M}_9 \\ \bar{V}_9 \\ \bar{F}_9 \end{array} \right\} \\
 \left. \begin{array}{c} \bar{u}_{10} \\ \bar{v}_{10} \\ \bar{\psi}_{10} \\ \bar{M}_{10} \\ \bar{V}_{10} \\ \bar{F}_{10} \end{array} \right\}
 \end{array} \right\} = \left. \begin{array}{c} 0 \\ 0 \\ 0 \\ 0 \\ 0 \\ 0 \\ 0 \\ 0 \\ 0 \end{array} \right\} \quad (A30)$$

The 9 x 18 matrix in eqn. (A30) is the joint coupling matrix \underline{B}_4 of joint 4.

Joints 5, 7 and 9

The geometry of each of joints 5, 7 and 9 is identical to the geometry of joint 3. Also, the relative directions of the local coordinate directions of the members attached to each of joints 5, 7 and 9 are identical to the relative directions of the members attached to joint 3. Therefore, each of the joint coupling matrices \underline{B}_5 , \underline{B}_7 and \underline{B}_9 is equal to \underline{B}_3 .

Joints 6, 8 and 10

The geometry of each of joints 6, 8 and 10 is identical to the geometry of joint 4. Also, the relative directions of the local coordinate directions of the members attached to each of joints 6, 8 and 10 are identical to the relative directions of the members attached to joint 4. Therefore, each of the joint coupling matrices \underline{B}_6 , \underline{B}_8 and \underline{B}_{10} is equal to \underline{B}_4 .

Joint 11

The components of the state vectors \underline{z}_{29} and \underline{z}_{30} and a free-body diagram of joint 11 are shown in Fig. A7. The equilibrium equations for joint 11 are

$$\begin{bmatrix} 1 & 0 & 0 \\ 0 & 1 & 0 \\ 0 & 0 & 1 \end{bmatrix} \begin{Bmatrix} M_{29} \\ V_{29} \\ F_{29} \end{Bmatrix} + \begin{bmatrix} -1 & 0 & 0 \\ 0 & 0 & -1 \\ 0 & 1 & 0 \end{bmatrix} \begin{Bmatrix} M_{30} \\ V_{30} \\ F_{30} \end{Bmatrix} = \begin{Bmatrix} 0 \\ 0 \\ 0 \end{Bmatrix} \quad (\text{A31})$$

The compatibility equations for joint 11 are

$$\begin{bmatrix} 1 & 0 & 0 \\ 0 & 1 & 0 \\ 0 & 0 & 1 \end{bmatrix} \begin{Bmatrix} u_{29} \\ v_{29} \\ \psi_{29} \end{Bmatrix} + \begin{bmatrix} 0 & -1 & 0 \\ 1 & 0 & 0 \\ 0 & 0 & -1 \end{bmatrix} \begin{Bmatrix} u_{30} \\ v_{30} \\ \psi_{30} \end{Bmatrix} = \begin{Bmatrix} 0 \\ 0 \\ 0 \end{Bmatrix} \quad (\text{A32})$$

Combining eqns. (A31) and (A32) and taking the Fourier transform of the resulting equation give

$$\begin{bmatrix} 1 & 0 & 0 & 0 & 0 & 0 & 0 & -1 & 0 & 0 & 0 & 0 \\ 0 & 1 & 0 & 0 & 0 & 0 & 1 & 0 & 0 & 0 & 0 & 0 \\ 0 & 0 & 1 & 0 & 0 & 0 & 0 & 0 & -1 & 0 & 0 & 0 \\ 0 & 0 & 0 & 1 & 0 & 0 & 0 & 0 & 0 & -1 & 0 & 0 \\ 0 & 0 & 0 & 0 & 1 & 0 & 0 & 0 & 0 & 0 & 0 & -1 \\ 0 & 0 & 0 & 0 & 0 & 1 & 0 & 0 & 0 & 0 & 1 & 0 \end{bmatrix} \begin{Bmatrix} \bar{u}_{29} \\ \bar{v}_{29} \\ \bar{\psi}_{29} \\ \bar{M}_{29} \\ \bar{V}_{29} \\ \bar{F}_{29} \\ \bar{u}_{30} \\ \bar{v}_{30} \\ \bar{\psi}_{30} \\ \bar{M}_{30} \\ \bar{V}_{30} \\ \bar{F}_{30} \end{Bmatrix} = \begin{Bmatrix} 0 \\ 0 \\ 0 \\ 0 \\ 0 \\ 0 \\ 0 \end{Bmatrix} \quad (\text{A33})$$

The 6 x 12 matrix in eqn. (A33) is the joint coupling matrix \underline{B}_{11} of joint 11.

Joint 12

The components of the state vectors \underline{z}_{31} and \underline{z}_{32} and a free-body diagram of joint 12 are shown in Fig. A8. The equilibrium equations for joint 12 are

$$\begin{bmatrix} 1 & 0 & 0 \\ 0 & 1 & 0 \\ 0 & 0 & 1 \end{bmatrix} \begin{Bmatrix} M_{31} \\ V_{31} \\ F_{31} \end{Bmatrix} + \begin{bmatrix} 1 & 0 & 0 \\ 0 & 0 & -1 \\ 0 & 1 & 0 \end{bmatrix} \begin{Bmatrix} M_{32} \\ V_{32} \\ F_{32} \end{Bmatrix} = \begin{Bmatrix} 0 \\ 0 \\ 0 \end{Bmatrix} \quad (\text{A34})$$

The compatibility equations for joint 12 are

$$\begin{bmatrix} 1 & 0 & 0 \\ 0 & 1 & 0 \\ 0 & 0 & 1 \end{bmatrix} \begin{Bmatrix} u_{31} \\ v_{31} \\ \psi_{31} \end{Bmatrix} + \begin{bmatrix} 0 & 1 & 0 \\ -1 & 0 & 0 \\ 0 & 0 & -1 \end{bmatrix} \begin{Bmatrix} u_{32} \\ v_{32} \\ \psi_{32} \end{Bmatrix} = \begin{Bmatrix} 0 \\ 0 \\ 0 \end{Bmatrix} \quad (\text{A35})$$

Combining eqns. (A34) and (A35) and taking the Fourier transform of the resulting equation give

$$\begin{bmatrix}
 1 & 0 & 0 & 0 & 0 & 0 & 0 & 1 & 0 & 0 & 0 & 0 \\
 0 & 1 & 0 & 0 & 0 & 0 & -1 & 0 & 0 & 0 & 0 & 0 \\
 0 & 0 & 1 & 0 & 0 & 0 & 0 & 0 & -1 & 0 & 0 & 0 \\
 0 & 0 & 0 & 1 & 0 & 0 & 0 & 0 & 0 & 1 & 0 & 0 \\
 0 & 0 & 0 & 0 & 1 & 0 & 0 & 0 & 0 & 0 & 0 & -1 \\
 0 & 0 & 0 & 0 & 0 & 1 & 0 & 0 & 0 & 0 & 1 & 0
 \end{bmatrix}
 \begin{Bmatrix}
 \bar{u}_{31} \\
 \bar{v}_{31} \\
 \bar{\psi}_{31} \\
 \bar{M}_{31} \\
 \bar{v}_{31} \\
 \bar{F}_{31} \\
 \bar{u}_{32} \\
 \bar{v}_{32} \\
 \bar{\psi}_{32} \\
 \bar{M}_{32} \\
 \bar{v}_{32} \\
 \bar{F}_{32}
 \end{Bmatrix}
 =
 \begin{Bmatrix}
 0 \\
 0 \\
 0 \\
 0 \\
 0 \\
 0 \\
 0 \\
 0 \\
 0 \\
 0 \\
 0 \\
 0
 \end{Bmatrix}
 \tag{A36}$$

The 6 x 12 matrix in eqn. (A36) is the joint coupling matrix \underline{B}_{12} of joint 12.

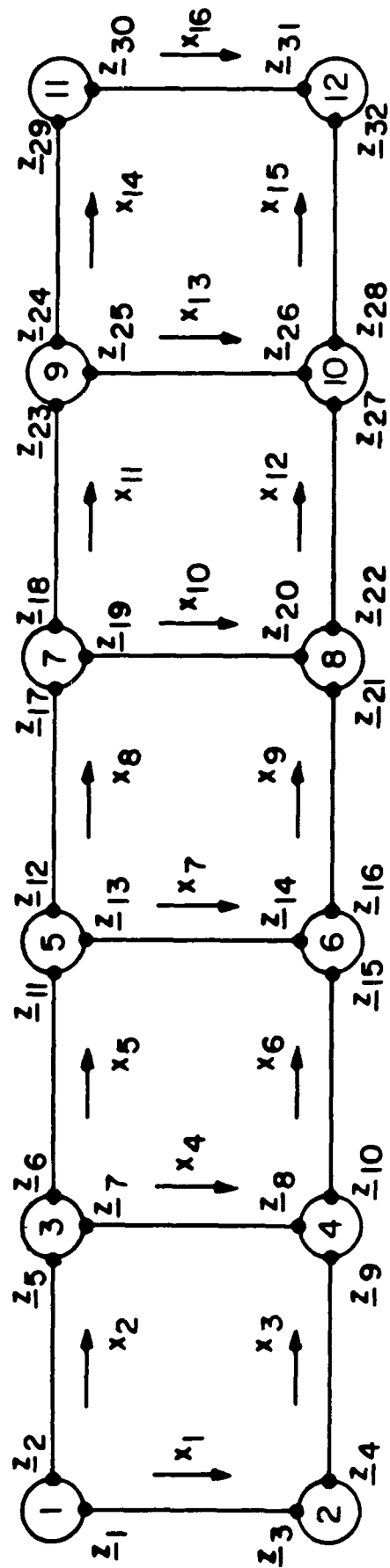


Fig. A1 Lattice model.

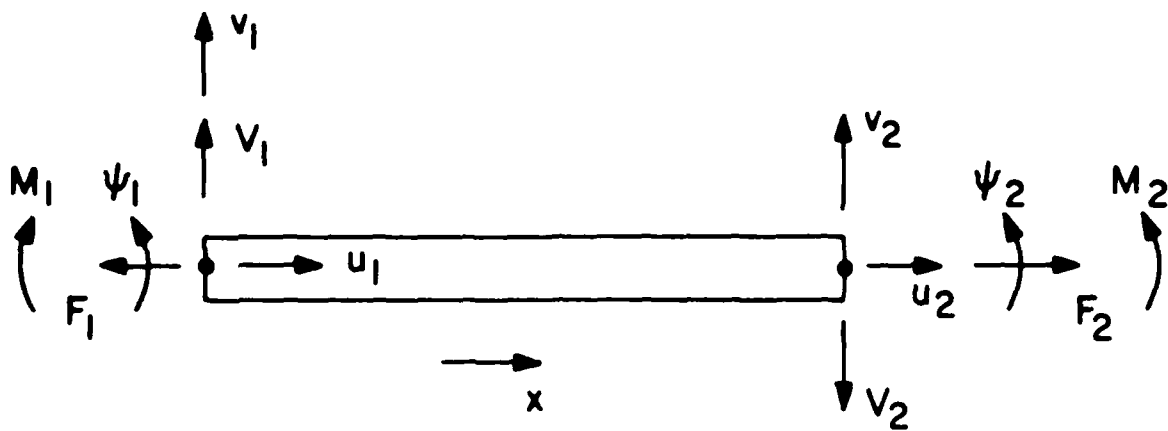


Fig. A2 Lattice member, showing components of state vectors and sign convention.

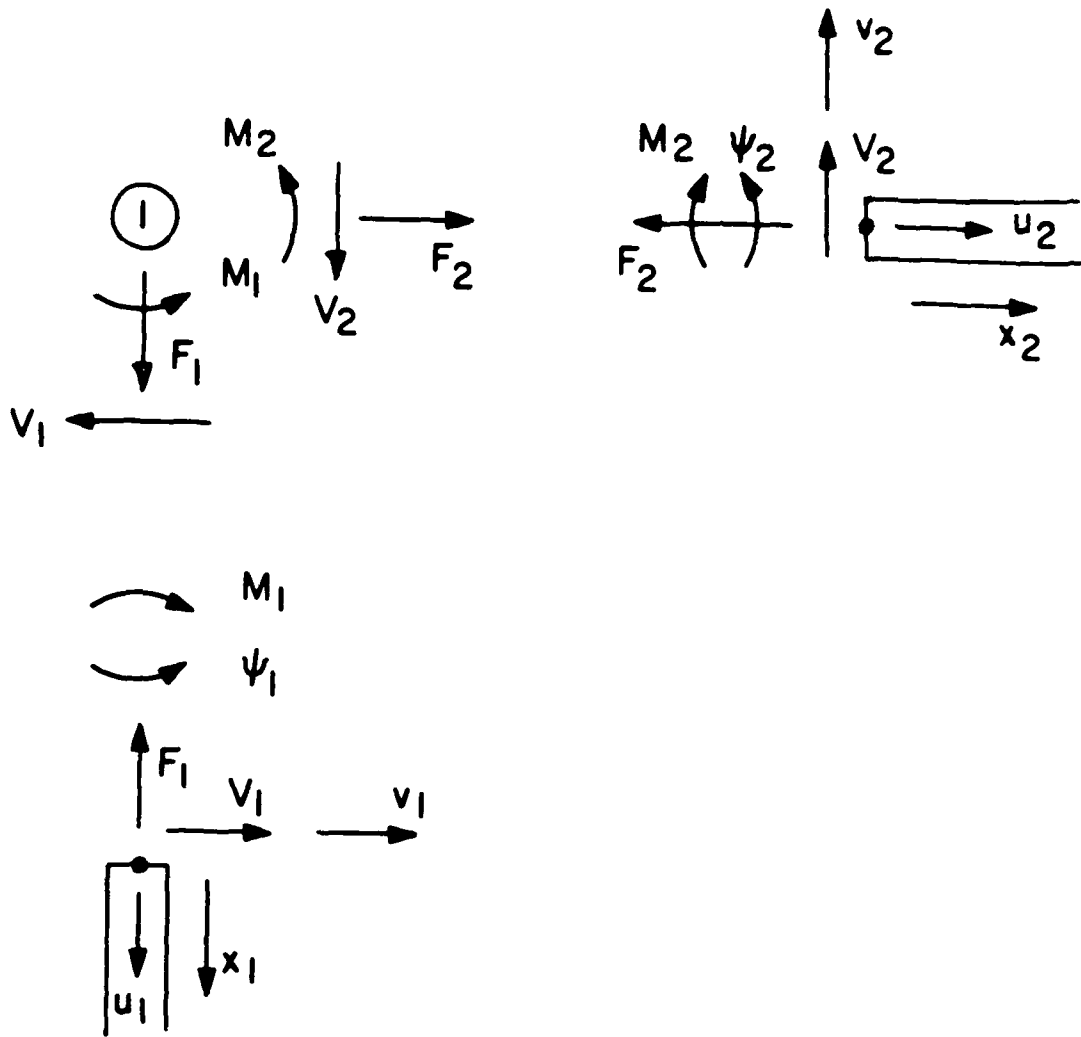


Fig. A3 Components of state vectors \underline{z}_1 and \underline{z}_2 , and free-body diagram of joint 1.

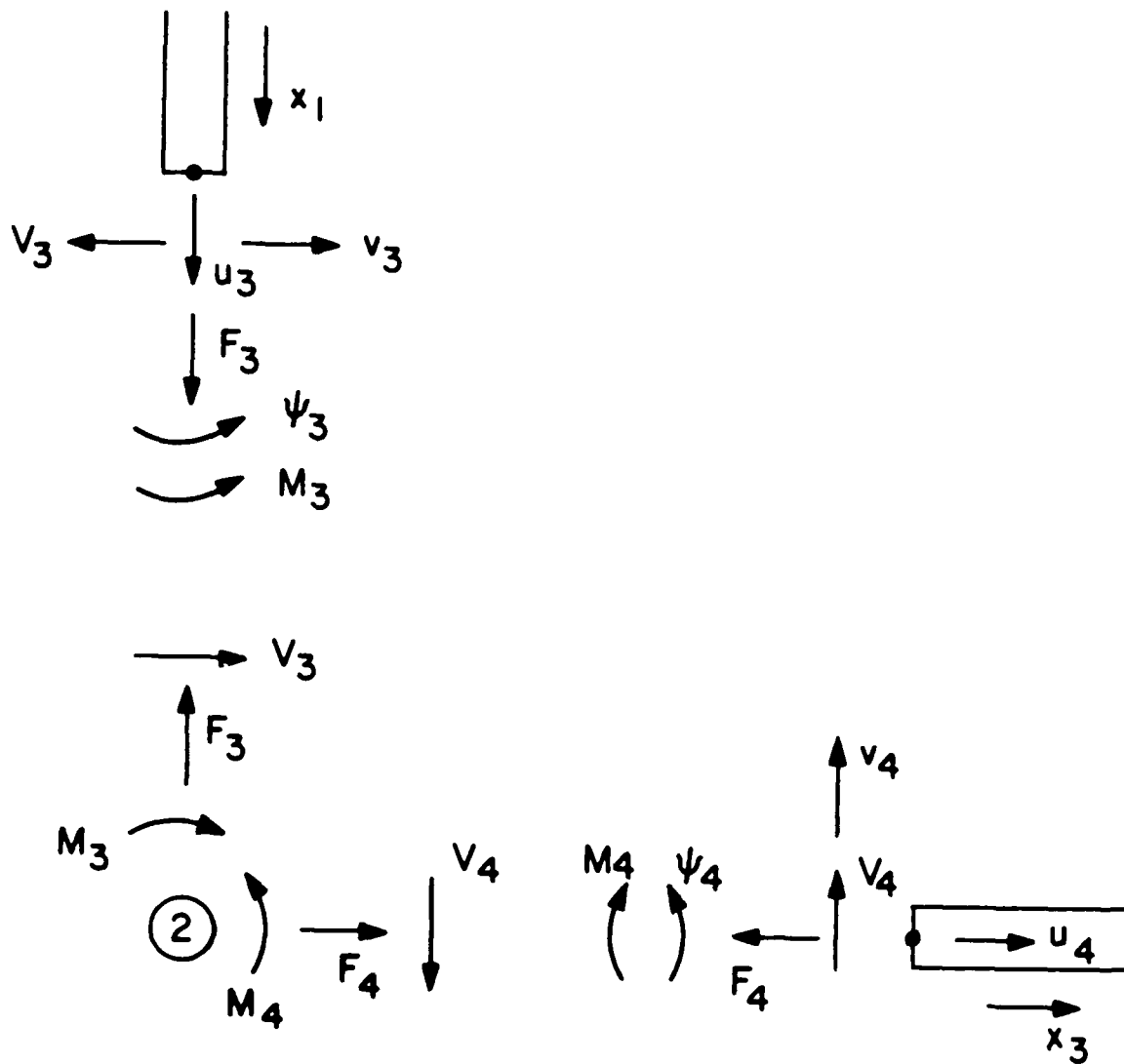


Fig. A4 Components of state vectors \underline{z}_3 and \underline{z}_4 , and free-body diagram of joint 2.

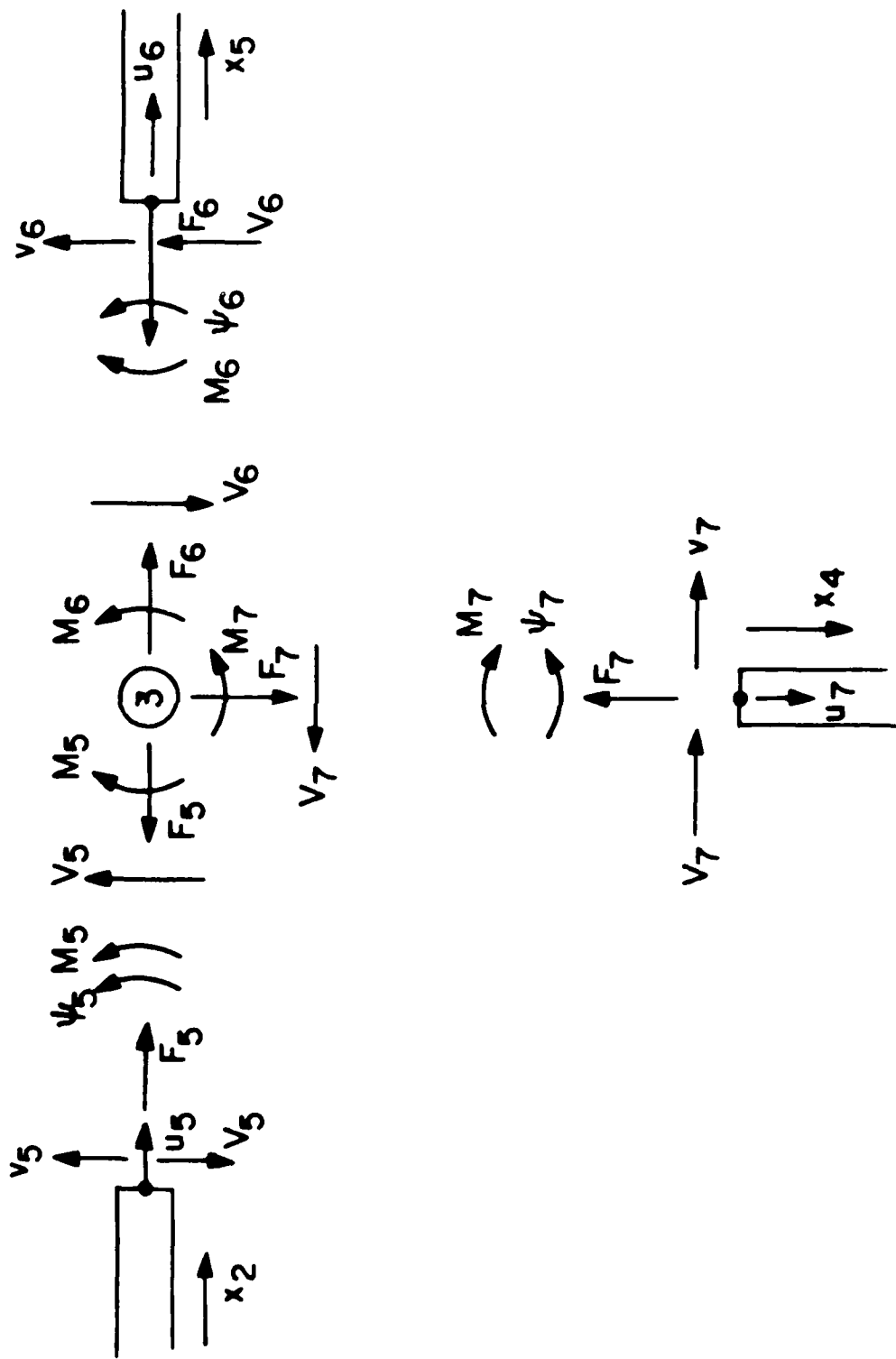


Fig. A5 Components of state vectors z_5 , z_6 and z_7 , and free-body diagram of joint 3.

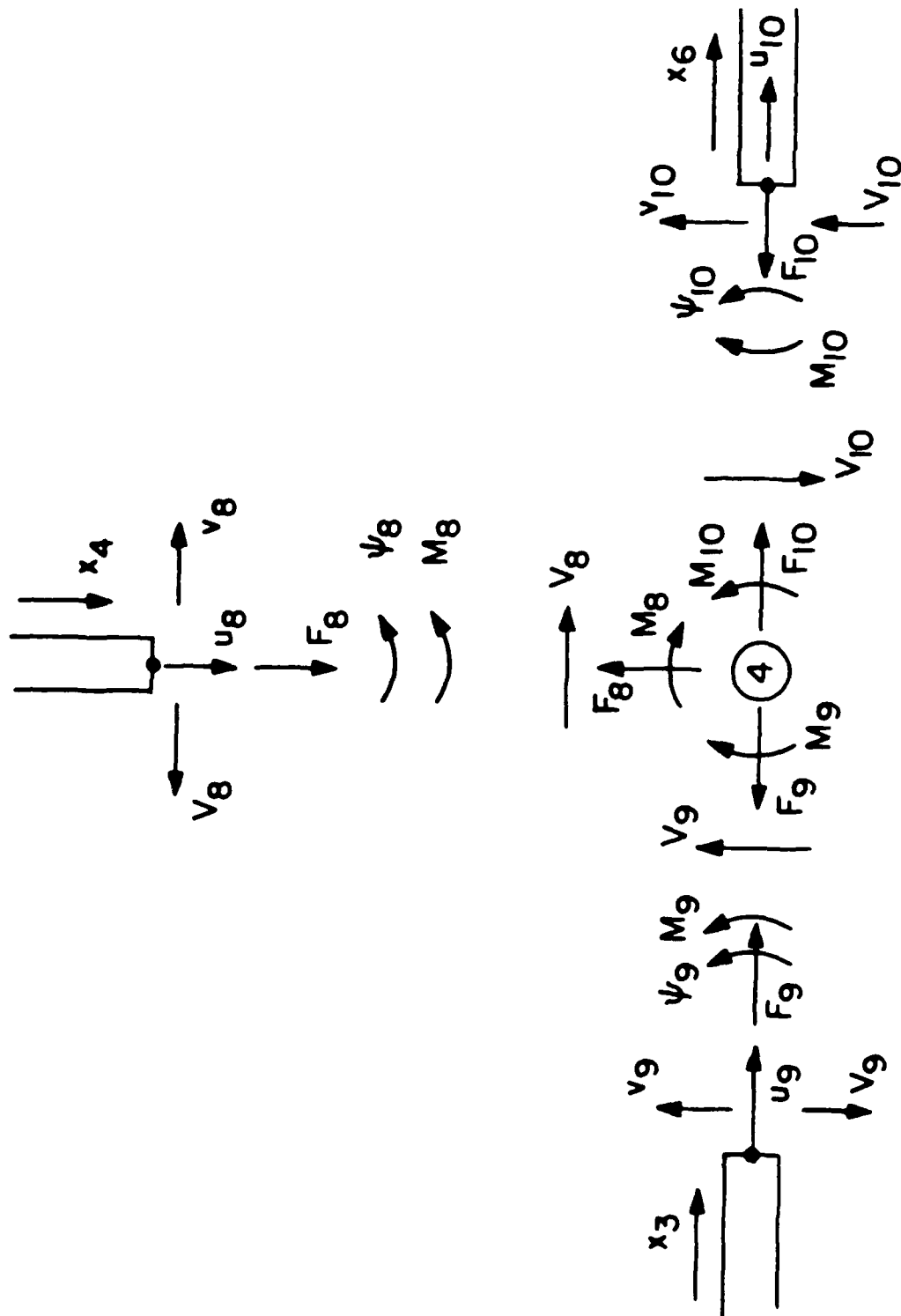


Fig. A6 Components of state vectors z_8 , z_9 and z_{10} , and free-body diagram of joint 4.

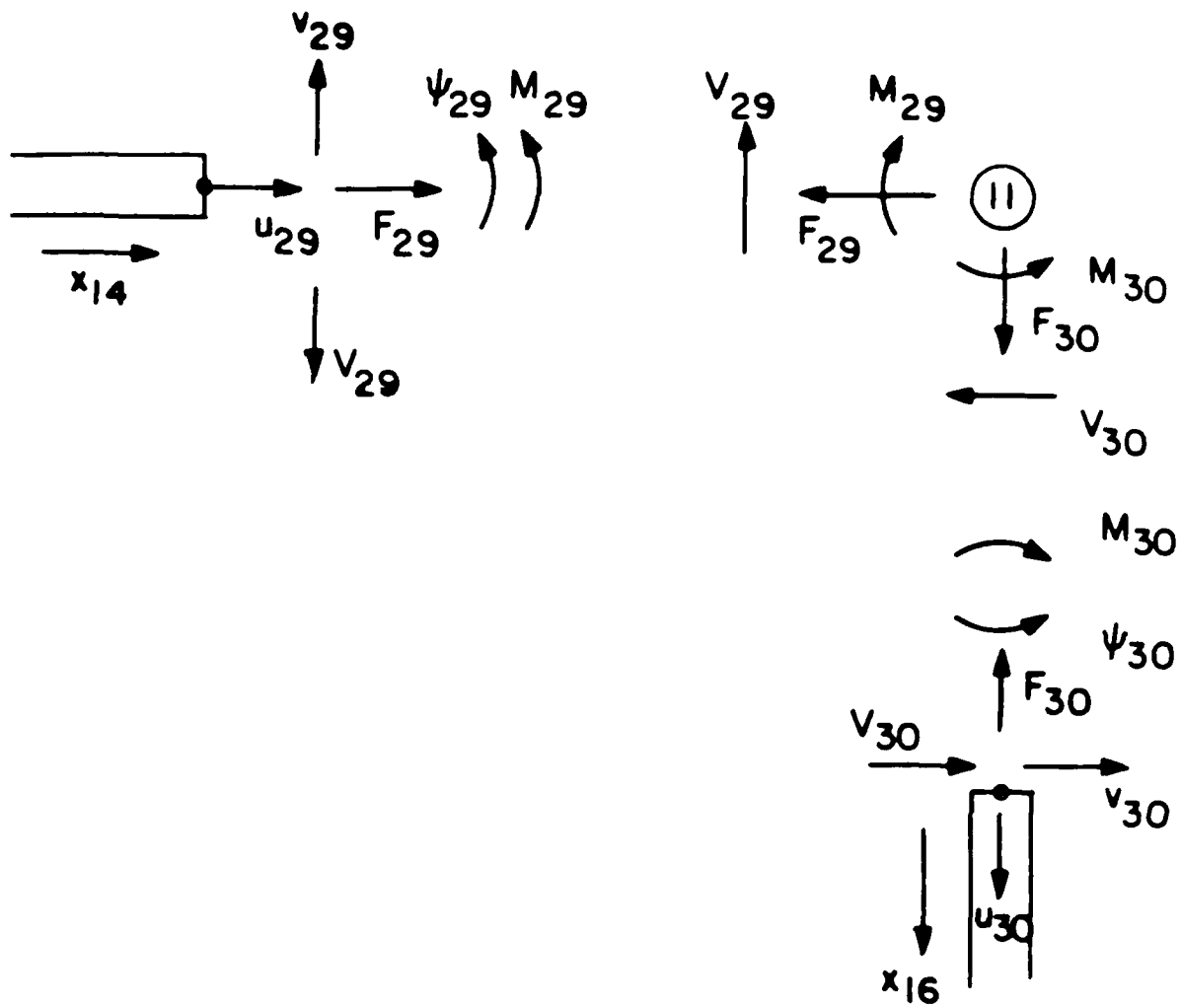


Fig. A7 Components of state vectors \underline{z}_{29} and \underline{z}_{30} , and free-body diagram of joint 11.

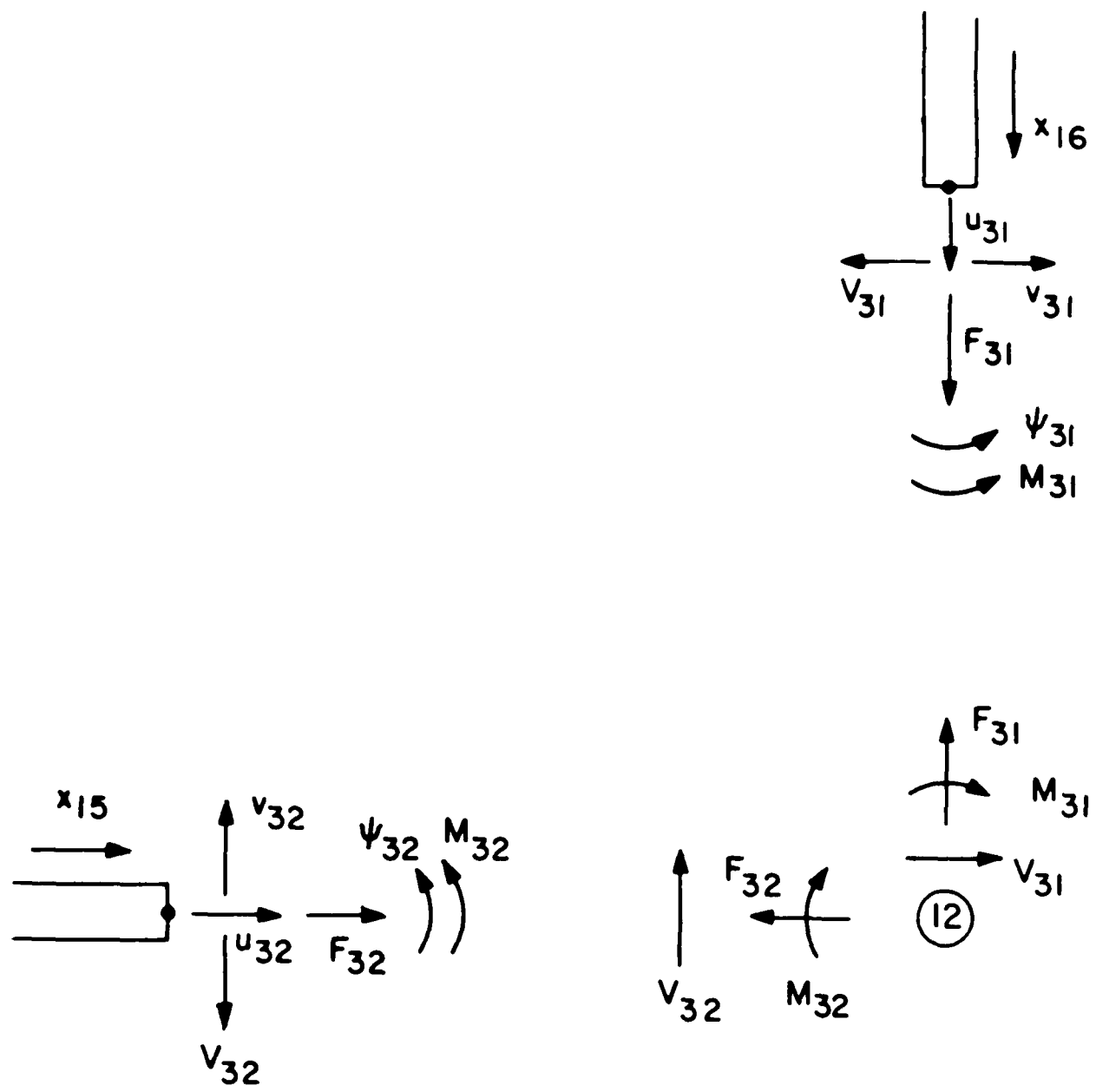


Fig. A8 Components of state vectors \underline{z}_{31} and \underline{z}_{32} , and free-body diagram of joint 12.

APPENDIX B: TRANSFER MATRIX RELATIONSHIPS

In this appendix, the transfer matrix relationships for two lattice member models are given. In the first model, hereafter called the Bernoulli-Euler beam model, the lattice member is modeled as a classical longitudinal rod for axial motions and as a Bernoulli-Euler beam for flexural motions. In the second model, hereafter called the Timoshenko beam model, the lattice member is modeled as a classical longitudinal rod for axial motions and as a Timoshenko beam for flexural motions. It is assumed in both models that the axial and flexural motions are uncoupled. For both models, the state vector at any point x of the lattice member is of the form

$$\underline{z}(x,t) = \begin{Bmatrix} u(x,t) \\ v(x,t) \\ \psi(x,t) \\ M(x,t) \\ V(x,t) \\ F(x,t) \end{Bmatrix} \quad (B1)$$

where $u(x,t)$ is the longitudinal displacement of the member, $v(x,t)$ is the transverse displacement of the member, $\psi(x,t)$ is the rotation of the member, $M(x,t)$ is the bending moment in the member, $V(x,t)$ is the shear force in the member, $F(x,t)$ is the axial force in the member, x is a spatial coordinate which extends along the length of the member and t is time. The components of the state vector and the sign convention adopted here for the components of the state vector are shown in Fig. B1. In Fig. B1, the left end of the member is designated as point 1, and the right end of the

member is designated as point 2. The local coordinate x is defined as shown in Fig. B1. Throughout this appendix, an overbar will denote a Fourier transform. Derivations of the transfer matrix relationships given here can be found in [1] and [11].

Bernoulli-Euler Beam Model

The transfer matrix relationship for the Bernoulli-Euler beam model is given by

$$\begin{Bmatrix} \bar{u}_1 \\ \bar{v}_1 \\ \bar{\psi}_1 \\ \bar{M}_1 \\ \bar{V}_1 \\ \bar{F}_1 \end{Bmatrix} = \begin{bmatrix} \cos\theta & 0 & 0 & 0 & 0 & 0 \\ 0 & c_0 & \ell c_1 & \ell^2 c_2 & 0 & \frac{\ell \sin\theta}{EA} \\ 0 & \frac{\beta^4 EI}{\ell^3} c_3 & c_0 & \frac{\ell c_1}{EI} & \frac{\ell^3 c_2}{EI} & 0 \\ 0 & \frac{\beta^4 EI}{\ell^2} c_2 & \frac{\beta^4 EI}{\ell} c_3 & c_0 & \frac{\ell c_1}{EI} & 0 \\ 0 & \frac{\beta^4 EI}{\ell^3} c_1 & \frac{\beta^4 EI}{\ell^2} c_2 & \frac{\beta^4 EI}{\ell} c_3 & \ell c_1 & 0 \\ 0 & \frac{-11\theta\omega^2 \sin\theta}{\theta} & 0 & 0 & 0 & \cos\theta \end{bmatrix} \begin{Bmatrix} \bar{u}_2 \\ \bar{v}_2 \\ \bar{\psi}_2 \\ \bar{M}_2 \\ \bar{V}_2 \\ \bar{F}_2 \end{Bmatrix} \quad (B2)$$

where

$$c_0 = \frac{1}{2} (\cosh\beta + \cos\beta) \quad (B3)$$

$$c_1 = \frac{1}{2\beta} (\sinh\beta + \sin\beta) \quad (B4)$$

$$c_2 = \frac{1}{2\beta^2} (\cosh\beta - \cos\beta) \quad (B5)$$

$$c_3 = \frac{1}{2\beta^3} (\sinh\beta - \sin\beta) \quad (B6)$$

$$\beta^4 = \frac{\mu\omega^2 \ell^4}{EI} \quad (B7)$$

$$\theta = \ell\omega\sqrt{\frac{\rho}{E}} \quad (B8)$$

In eqns. (B2) through (B8), μ is the mass per unit length of the member, ω is radian frequency, ℓ is the length of the member from point 1 to point 2, E is the elastic modulus of the member, EI is the flexural rigidity of the member, A is the cross-sectional area of the member and ρ is the mass density (mass per unit volume) of the member. For numerical computations, the following values of the material and geometric constants are used:

$\mu = 2.44 \times 10^{-5} \text{ lb-sec}^2/\text{in}^2$, $\ell = 9.85 \text{ in}$, $E = 10 \times 10^6 \text{ lb/in}^2$, $EI = 4880 \text{ lb-in}^2$, $A = 9.38 \times 10^{-2} \text{ in}^2$ and $\rho = 2.6 \times 10^{-4} \text{ lb-sec}^2/\text{in}^4$.

Timoshenko Beam Model

The transfer matrix relationship for the Timoshenko beam model is given by

$$\begin{bmatrix}
 \bar{u}_2 \\
 \bar{v}_2 \\
 \bar{\psi}_2 \\
 \bar{M}_2 \\
 \bar{V}_2 \\
 \bar{F}_2
 \end{bmatrix}
 =
 \begin{bmatrix}
 \cos\theta & 0 & 0 & 0 & 0 & -\frac{\mu\ell\omega^2 \sin\theta}{\theta} \\
 0 & c_0^{-\sigma c_2} & \ell [c_1 - (\sigma + \tau)c_3] & 0 & 0 & 0 \\
 0 & \frac{\beta^4}{\ell} c_3 & c_0^{-\tau c_2} & \frac{\ell(c_1 - \tau c_3)}{EI} & 0 & 0 \\
 0 & \frac{\beta^4 EI}{\ell^2} c_2 & \frac{EI}{\ell} [-\tau c_1 + (\beta^4 + \tau^2)c_3] & c_0^{-\tau c_2} & 0 & 0 \\
 0 & \frac{\beta^4 EI}{\ell^3} (c_1 - \sigma c_3) & \frac{\beta^4 EI}{\ell^2} c_2 & \frac{\beta^4}{\ell} c_3 & c_0^{-\sigma \tau_2} & 0 \\
 -\frac{\mu\ell\omega^2 \sin\theta}{\theta} & 0 & 0 & 0 & 0 & \cos\theta
 \end{bmatrix}
 \begin{bmatrix}
 \bar{u}_1 \\
 \bar{v}_1 \\
 \bar{\psi}_1 \\
 \bar{M}_1 \\
 \bar{V}_1 \\
 \bar{F}_1
 \end{bmatrix}
 \quad (B9)$$

where

$$c_0 = \Lambda(\lambda_2^2 \cosh \lambda_1 + \lambda_1^2 \cos \lambda_2) \quad (\text{B10})$$

$$c_1 = \Lambda \left(\frac{\lambda_2^2}{\lambda_1} \sinh \lambda_1 + \frac{\lambda_1^2}{\lambda_2} \sin \lambda_2 \right) \quad (\text{B11})$$

$$c_2 = \Lambda(\cosh \lambda_1 - \cos \lambda_2) \quad (\text{B12})$$

$$c_3 = \Lambda \left(\frac{\sinh \lambda_1}{\lambda_1} - \frac{\sin \lambda_2}{\lambda_2} \right) \quad (\text{B13})$$

$$\Lambda = \frac{1}{\lambda_1^2 + \lambda_2^2} \quad (\text{B14})$$

$$\lambda_1 = \sqrt{\sqrt{\beta^4 + \frac{1}{4}(\sigma - \tau)^2} - \frac{1}{2}(\sigma + \tau)} \quad (\text{B15})$$

$$\lambda_2 = \sqrt{\sqrt{\beta^4 + \frac{1}{4}(\sigma - \tau)^2} + \frac{1}{2}(\sigma + \tau)} \quad (\text{B16})$$

$$\sigma = \frac{\mu \omega^2 \ell^2}{GA_s} \quad (\text{B17})$$

$$\tau = \frac{\mu I_y^2 \omega^2 \ell^2}{EI} \quad (\text{B18})$$

$$\theta = \ell \omega \sqrt{\frac{\rho}{E}} \quad (\text{B19})$$

$$\beta^4 = \frac{\mu \omega^2 \ell^4}{EI} \quad (\text{B20})$$

In eqns. (B9) through (B20), μ is the mass per unit length of the member, ω is radian frequency, ℓ is the length of the member from point 1 to point 2, G is the shear modulus of the member, A_s is the cross-sectional area of the member divided by the geometric correction factor κ , i_y is the radius of gyration of the member cross section, EI is the flexural rigidity of the member, ρ is the mass density (mass per unit volume) of the member, E is the elastic modulus of the member and A is the cross-sectional area of the member. For numerical computations, the following values of the material and geometric constants are used: $\mu = 2.44 \times 10^{-5}$ lb-sec²/in², $\ell = 9.85$ in, $G = 3.8 \times 10^6$ lb/in², $A_s = 0.113$ in², $\kappa = 0.833$, $i_y = 7.21 \times 10^{-2}$ in, $EI = 4880$ lb-in², $\rho = 2.6 \times 10^{-4}$ lb-sec²/in⁴, $E = 10 \times 10^6$ lb/in² and $A = 9.38 \times 10^{-2}$ in².

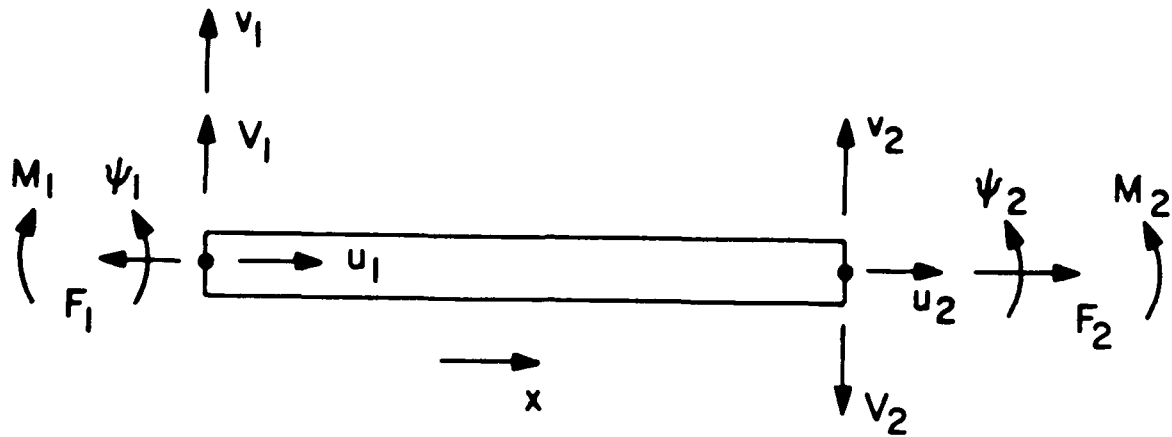


Fig. B1 Lattice member, showing components of state vectors and sign convention.

APPENDIX C: LISTING OF COMPUTER PROGRAM

```

PROGRAM detcalc (input,output);

(* This program is used to evaluate det(BG(w)TG(w)) for a *)
(* given value of w. The nonzero elements of BG(w)TG(w) are *)
(* stored in the matrix STBG TG. The matrix DIAG contains *)
(* the nonzero diagonal lines of BG(w)TG(w). The matrix *)
(* DIAG is passed to the procedure bandet, which returns *)
(* the value of det(BG(w)TG(w)). A discussion of the *)
(* procedure bandet is given in Linear Algebra, by J. H. *)
(* Wilkinson and C. Reinsch, Springer-Verlag, 1971. *)

CONST
  m = 6;
  n = 96;
  p = 36;
  m1 = 23;
  m2 = 17;
  E = 10E6;
  G = 3.8E6;
  lth = 9.85;
  ro = 2.6E-4;
  kap = 0.8333;
  EI = 4880;
  ar = 0.0938;
  AS = 0.1126;
  mu = 2.439E-5;
  r = 0.0721;

TYPE
  mmatrix = ARRAY [1..m,1..m] OF real;
  npmatrix = ARRAY [1..n,1..p] OF real;
  dmatrix = ARRAY [1..n,-m1..m2] OF real;

VAR
  th,w,b4,sig,tau,lam1,lam2,lam,c0,c1,c2,c3,det,b :real;
  STBG TG :nmatrix;
  DIAG :dmatrix;
  T,ID,B12,B22,B31,B32,B33,B34,B35,B36,B41,B42,
  B45,B46,B112,B122 :mmatrix;
  i,j,k :integer;
  Timoshenko, BernoulliEuler :Boolean;

PROCEDURE bandet(n,m1,m2:integer; VAR A:dmatrix; VAR det:real);

VAR
  d1,x,norm,macheps :real;
  i,j,k,l :integer;

```

```

BEGIN
macheps := 0.0000000000000001;
norm := 0.0;

FOR i := 1 to n DO
  BEGIN x := 0.0;
    FOR j := -m1 to m2 DO
      x := x + abs(A[i,j]);
      IF (norm < x) THEN norm := x;
    END;
  l := m1;
  FOR i := 1 to m1 DO
    BEGIN
      FOR j := 1-i to m2 DO
        A[i,j-1] := A[i,j];
        l := l - 1;
      FOR j := m2-1 to m2 DO
        A[i,j] := 0.0;
      END;
    d1 := 1.0; l := m1;
    FOR k := 1 to n DO
      BEGIN x := A[k,-m1]; i := k;
        IF (l < n) THEN l := l + 1;
        FOR j := k + 1 to l do
          IF abs(A[j,-m1]) > abs(x) THEN
            BEGIN x := A[j,-m1]; i := j; END;
          d1 := d1 * x;
          IF (x = 0) THEN
            BEGIN
              A[k,-m1] := norm * macheps;
            END;
          IF (i <> k) THEN
            BEGIN d1 := -d1;
              FOR j := -m1 to m2 DO
                BEGIN x := A[k,j]; A[k,j] := A[i,j];
                  A[i,j] := x;
                END;
              END;
            FOR i := k + 1 to l DO
              BEGIN x := A[i,-m1]/A[k,-m1];
                FOR j := 1-m1 to m2 DO
                  A[i,j-1] := A[i,j] - (x * A[k,j]);
                  A[i,m2] := 0;
                END;
              END;
            END;
          det := d1;
        END;
      FUNCTION sinh (x:real) : real;
        BEGIN
          sinh := (exp(x) - exp(-x))/2.0;
        END;

```

```

FUNCTION cosh (x:real) : real;
  BEGIN
    cosh := (exp(x) + exp(-x))/2.0
  END;

BEGIN

Timoshenko      := false;
BernoulliEuler := true;

FOR i := 1 to m DO      (* initialize submatrices of BGTG *)
  BEGIN
    FOR j := 1 to m DO
      BEGIN
        ID[i,j] := 0.0; B32[i,j] := 0.0;
        B12[i,j] := 0.0; B33[i,j] := 0.0;
        B22[i,j] := 0.0; B34[i,j] := 0.0;
        B31[i,j] := 0.0; B35[i,j] := 0.0;
        B36[i,j] := 0.0; B41[i,j] := 0.0;
        B42[i,j] := 0.0; B45[i,j] := 0.0;
        B46[i,j] := 0.0; B112[i,j] := 0.0;
        B122[i,j] := 0.0;
      END;
    END;

      (* form the joint coupling matrices *)

B12[1,2] := 1.0;   B12[4,4] := 1.0;
B12[2,1] := -1.0; B12[5,6] := -1.0;
B12[3,3] := -1.0; B12[6,5] := 1.0;
B22[1,2] := 1.0;   B22[4,4] := -1.0;
B22[2,1] := -1.0; B22[5,6] := 1.0;
B22[3,3] := -1.0; B22[6,5] := -1.0;
B31[1,1] := 1.0;   B31[4,1] := 1.0;
B31[2,2] := 1.0;   B31[5,2] := 1.0;
B31[3,3] := 1.0;   B31[6,3] := 1.0;
B32[1,1] := -1.0;  B33[4,2] := -1.0;
B32[2,2] := -1.0;  B33[5,1] := 1.0;
B32[3,3] := -1.0;  B33[6,3] := -1.0;
B34[1,4] := 1.0;   B35[1,4] := -1.0;
B34[2,5] := 1.0;   B35[2,5] := -1.0;
B34[3,6] := 1.0;   B35[3,6] := -1.0;
B36[1,4] := -1.0;  B41[4,1] := 1.0;
B36[2,6] := -1.0;  B41[5,2] := 1.0;
B36[3,5] := 1.0;   B41[6,3] := 1.0;
B42[4,2] := 1.0;   B45[4,4] := 1.0;
B42[5,1] := -1.0;  B45[5,6] := -1.0;
B42[6,3] := -1.0;  B45[6,5] := 1.0;
B46[1,2] := 1.0;   B46[4,4] := -1.0;
B46[2,1] := -1.0;  B46[5,6] := 1.0;
B46[3,3] := -1.0;  B46[6,5] := -1.0;

```

```

B112[1,2] := -1.0;   B112[4,4] := -1.0;
B112[2,1] :=  1.0;   B112[5,6] := -1.0;
B112[3,3] := -1.0;   B112[6,5] :=  1.0;
B122[1,2] :=  1.0;   B122[4,4] :=  1.0;
B122[2,1] := -1.0;   B122[5,6] := -1.0;
B122[3,3] := -1.0;   B122[6,5] :=  1.0;
ID[1,1]   :=  1.0;   ID[4,4]   :=  1.0;
ID[2,2]   :=  1.0;   ID[5,5]   :=  1.0;
ID[3,3]   :=  1.0;   ID[6,6]   :=  1.0;

w := 10.0;          (* assign a value to w *)

WHILE (w < 10000.0) DO
BEGIN
  FOR i := 1 to n DO      (* initialize the matrix STBGTG *)
  BEGIN
    FOR j := 1 to p DO
    BEGIN
      STBGTG[i,j] := 0.0;
    END;
  END;

  IF (Timoshenko) THEN
  BEGIN (* form transfer matrix of Timoshenko beam *)
    th := lth * w * sqrt(ro/E);
    b4 := mu * sqr(w) * sqr(sqr(lth))/EI;
    sig := mu * sqr(w) * sqr(lth)/(G*as);
    tau := mu * sqr(r) * sqr(w) * sqr(lth)/EI;
    lam1 := sqrt(sqrt(b4 + ((sqr(sig-tau))/4))
                - (sig+tau)/2);
    lam2 := sqrt(sqrt(b4 + ((sqr(sig-tau))/4))
                + (sig+tau)/2);
    lam := 1/(sqr(lam1) + sqr(lam2));
    c0 := lam * (sqr(lam2) * cosh(lam1)
                + sqr(lam1) * cos(lam2));
    c1 := lam * (sqr(lam2)/lam1 * sinh(lam1)
                + sqr(lam1)/lam2 * sin(lam2));
    c2 := lam * (cosh(lam1) - cos(lam2));
    c3 := lam * (1/lam1 * sinh(lam1)
                - 1/lam2 * sin(lam2));

    T[1,1] := cos(th);
    T[1,2] := 0.0;
    T[1,3] := 0.0;
    T[1,4] := 0.0;
    T[1,5] := 0.0;
    T[1,6] := lth/(E*ar)*sin(th)/th;
    T[2,1] := 0.0;
    T[2,2] := c0 - (sig*c2);
    T[2,3] := lth*(c1 - ((sig + tau) * c3));
    T[2,4] := (sqr(lth)/EI)*c2;
  END;
END;

```

```

T[2,5] := (sqr(lth)*lth/(b4*EI))*(-(sig*c1)
          + ((b4 + sqr(sig))*c3));
T[2,6] := 0.0;
T[3,1] := 0.0;
T[3,2] := (b4/lth)*c3;
T[3,3] := c0 - (tau*c2);
T[3,4] := (lth/EI) * (c1 - (tau*c3));
T[3,5] := T[2,4];
T[3,6] := 0.0;
T[4,1] := 0.0;
T[4,2] := b4 * (EI/sqr(lth)) * c2;
T[4,3] := (EI/lth) * (-(tau*c1) + ((b4 + sqr(tau))*c3));
T[4,4] := T[3,3];
T[4,5] := T[2,3];
T[4,6] := 0.0;
T[5,1] := 0.0;
T[5,2] := b4*(EI/(sqr(lth)*lth))*(c1 - (sig*c3));
T[5,3] := T[4,2];
T[5,4] := T[3,2];
T[5,5] := T[2,2];
T[5,6] := 0.0;
T[6,1] := -mu*lth*sqr(w)*sin(th)/th;
T[6,2] := 0.0;
T[6,3] := 0.0;
T[6,4] := 0.0;
T[6,5] := 0.0;
T[6,6] := cos(th);
END;

IF (BernoulliEuler) THEN
BEGIN (* form transfer matrix of Bernoulli-Euler beam *)
  b4 := mu * sqr(w) * sqr(sqr(lth)) / EI;
  b := sqrt(sqrt(b4));
  th := lth * w * sqrt(ro/E);
  c0 := 0.5 * (cosh(b) + cos(b));
  c1 := (1 / (2 * b)) * (sinh(b) + sin(b));
  c2 := (1 / (2 * sqr(b))) * (cosh(b) - cos(b));
  c3 := (1 / (2 * sqr(b) * b)) * (sinh(b) - sin(b));
  T[1,1] := cos(th);
  T[1,2] := 0.0;
  T[1,3] := 0.0;
  T[1,4] := 0.0;
  T[1,5] := 0.0;
  T[1,6] := lth / (E * ar) * sin(th) / th;
  T[2,1] := 0.0;
  T[2,2] := c0;
  T[2,3] := lth * c1;
  T[2,4] := sqr(lth) * c2 / EI;
  T[2,5] := sqr(lth) * lth * c3 / EI;
  T[2,6] := 0.0;
  T[3,1] := 0.0;

```

```

T[3,2] := b4 * c3 / lth;
T[3,3] := c0;
T[3,4] := lth * c1 / EI;
T[3,5] := T[2,4];
T[3,6] := 0.0;
T[4,1] := 0.0;
T[4,2] := b4 * EI * c2 / sqr(lth);
T[4,3] := b4 * EI * c3 / lth;
T[4,4] := T[3,3];
T[4,5] := T[2,3];
T[4,6] := 0.0;
T[5,1] := 0.0;
T[5,2] := b4 * EI * c1 / (sqr(lth) * lth);
T[5,3] := T[4,2];
T[5,4] := T[3,2];
T[5,5] := T[2,2];
T[5,6] := 0.0;
T[6,1] := -mu * lth * sqr(w) * sin(th) / th;
T[6,2] := 0.0;
T[6,3] := 0.0;
T[6,4] := 0.0;
T[6,5] := 0.0;
T[6,6] := cos(th);
END;

FOR i := 1 to m DO (* form the matrix STBGTG *)
BEGIN
  FOR j := 1 to m DO
  BEGIN
    STBGTG[ i , 18 + j ] := ID[i,j];
    STBGTG[ i , 24 + j ] := B12[i,j];
    STBGTG[ 6 + i, 12 + j ] := T[i,j];
    STBGTG[ 6 + i, 24 + j ] := B22[i,j];
    STBGTG[ 12 + i, 24 + j ] := B32[i,j];
    STBGTG[ 12 + i, 30 + j ] := B33[i,j];
    STBGTG[ 18 + i, 18 + j ] := B35[i,j];
    STBGTG[ 24 + i, 18 + j ] := T[i,j];
    STBGTG[ 24 + i, 24 + j ] := B46[i,j];
    STBGTG[ 30 + i, 24 + j ] := B32[i,j];
    STBGTG[ 30 + i, 30 + j ] := B33[i,j];
    STBGTG[ 36 + i, 18 + j ] := B35[i,j];
    STBGTG[ 84 + i, 6 + j ] := T[i,j];
    STBGTG[ 84 + i, 24 + j ] := B112[i,j];
    STBGTG[ 90 + i, 18 + j ] := T[i,j];
    FOR k := 1 to m DO
    BEGIN
      STBGTG[ 12 + i, 12 + j ] := STBGTG[ 12 + i, 12 + j ]
        + B31[i,k] * T[k,j];
      STBGTG[ 18 + i, 6 + j ] := STBGTG[ 18 + i, 6 + j ]
        + B34[i,k] * T[k,j];
    END;
  END;
END;

```

```

        STBGTG[18 + i, 12 + j] := STBGTG[18 + i, 12 + j]
                                + B42[i,k] * T[k,j];
        STBGTG[18 + i, 24 + j] := STBGTG[18 + i, 24 + j]
                                + B41[i,k] * T[k,j];
        STBGTG[24 + i, 6 + j] := STBGTG[24 + i, 6 + j]
                                + B45[i,k] * T[k,j];
        STBGTG[90 + i, 12 + j] := STBGTG[90 + i, 12 + j]
                                + B122[i,k] * T[k,j];
    END;
    STBGTG[18 + i, 24 + j] := STBGTG[18 + i, 24 + j]
                            + B36[i,j];
    STBGTG[30 + i, 6 + j] := STBGTG[12 + i, 12 + j];
    STBGTG[36 + i, j] := STBGTG[18 + i, 6 + j];
    STBGTG[36 + i, 12 + j] := STBGTG[18 + i, 12 + j];
    STBGTG[36 + i, 24 + j] := STBGTG[18 + i, 24 + j];
END;
END;
FOR i := 1 to m DO
BEGIN
    FOR j := 1 to p DO
        BEGIN
            STBGTG[42 + i,j] := STBGTG[24 + i,j];
            STBGTG[48 + i,j] := STBGTG[30 + i,j];
            STBGTG[54 + i,j] := STBGTG[36 + i,j];
            STBGTG[60 + i,j] := STBGTG[24 + i,j];
            STBGTG[66 + i,j] := STBGTG[30 + i,j];
            STBGTG[72 + i,j] := STBGTG[36 + i,j];
            STBGTG[78 + i,j] := STBGTG[24 + i,j];
        END;
    END;
END;

FOR i := 1 to n DO (* initialize the matrix DIAG *)
    BEGIN
        FOR j := -m1 to m2 DO
            BEGIN
                DIAG[i,j] := 0.0;
            END;
        END;
    END;

FOR i := 0 to 95 DO (* form the matrix DIAG *)
    BEGIN
        FOR j := 1 to 36 DO
            BEGIN
                DIAG[i + 1, -19 - (i mod 6) + j] := STBGTG[i + 1, j];
            END;
        END;
    END;

write (Lst,w);
bandet(n,m1,m2,DIAG,det); (* call procedure bandet, *)
writeln (Lst,det); (* write det, *)
w := w + 10.0; (* and add an increment to w *)
END;
END.

```

END

11-87

DTIC